

BEC-BCS Crossover in the Nambu–Jona-Lasinio Model of QCD

Gao Feng Sun*, Lianyi He† and Pengfei Zhuang‡
Physics Department, Tsinghua University, Beijing 100084, China

The BEC-BCS crossover in QCD at finite baryon and isospin chemical potentials is investigated in the Nambu–Jona-Lasinio model. The diquark condensation in two color QCD and the pion condensation in real QCD would undergo a BEC-BCS crossover when the corresponding chemical potential increases. We determined the crossover chemical potential as well as the BEC and BCS regions. The crossover is not triggered by increasing the strength of attractive interaction among quarks but driven by changing the charge density. The chiral symmetry restoration at finite temperature and density plays an important role in the BEC-BCS crossover. For real QCD, strong couplings in diquark and vector meson channels can induce a diquark BEC-BCS crossover in color superconductor, and in the BEC region the chromomagnetic instability is fully cured and the ground state is a uniform phase.

PACS numbers: 11.30.Qc, 12.38.Lg, 11.10.Wx, 25.75.Nq

I. INTRODUCTION

There exists a rich phase structure of Quantum Chromodynamics (QCD), for instance, the deconfinement process from hadron gas to quark-gluon plasma and the transition from chiral symmetry breaking to the symmetry restoration[1] at high temperature and/or baryon density, the color superconductivity at low temperature but high baryon density[2, 3], and the pion superfluidity at low temperature but high isospin density[4]. The physical motivation to study the QCD phase diagram is closely related to the investigation of early universe, compact stars and relativistic heavy ion collisions.

While the perturbation theory of QCD can well describe the properties of the new phases at high temperature and/or high density, the study on the phase transitions themselves at moderate temperature and density depends on lattice QCD calculation and effective models with QCD symmetries. While there is not yet precise lattice result for real QCD at finite baryon density due to the fermion sign problem[5], it is in principle no problem to do lattice simulation for two color QCD at finite baryon density[6, 7, 8, 9] and real QCD at finite isospin density[10, 11, 12]. The QCD phase transitions at finite baryon and/or isospin chemical potential are also investigated in many low energy effective models, such as chiral perturbation theory[13, 14, 15, 16, 17, 18, 19, 20], linear sigma model[21, 22, 23], Nambu–Jona-Lasinio model[24, 25, 26, 27, 28, 29, 30, 31], random matrix model[32, 33], ladder QCD[34], strong coupling lattice QCD[35], and global color model[36].

It is generally expected that there would exist a crossover from Bose-Einstein condensation(BEC) to Bardeen-Cooper-Schrieffer condensation(BCS) for diquarks at finite baryon density and pions at finite isospin

density. In the chemical potential region above but close to the critical value μ_c for diquark condensate in two color QCD or pion condensate in real QCD, since the deconfinement does not yet happen, the system should be in the BEC state of diquarks or pions. On the other hand, at a sufficiently high chemical potential $\mu >> \mu_c$, the ground state of the system becomes a BCS superfluid where quark-quark or quark-antiquark cooper pairs are condensed. Therefore, there should be a crossover from BEC state to BCS state when the chemical potential or density increases. The BEC-BCS crossover, which is a hot topic in and beyond condensed matter and ultracold fermion gas[37, 38, 39, 40, 41, 42, 43], was recently extended to relativistic fermion superfluid[44, 45, 46]. In these studies, the BEC-BCS crossover is induced by increasing the attractive coupling among fermions. However, this is not the only way to trigger BEC-BCS crossover. In this paper, we will study the BEC-BCS crossover induced by density effect and chiral symmetry restoration. This density induced BEC-BCS crossover is like the one found in nuclear matter[47] and non-dilute fermi gas[48].

The features of BEC-BCS crossover have been widely discussed in condensed matter and ultracold fermion gas[37, 38, 39, 40, 41, 42]. We list here only the essential characteristics:

- 1) There exist two important temperatures, one is the phase transition temperature T_c for the superfluid at which the order parameter vanishes, and the other is the molecule dissociation temperature T^* . In the BCS limit, there exists no stable molecule, and T^* approaches to T_c . In the BEC limit, all fermions form stable dimeron molecules, and T^* becomes much larger than T_c .
- 2) The chemical potential is equal to the Fermi energy of non-interacting fermion gas in the BCS limit but becomes negative in the BEC region. In the BEC limit, the absolute value of the chemical potential tends to be half of the molecule binding energy. This is true both near the critical temperature and in the superfluid ground state.
- 3) The fermion momentum distribution changes significantly when we go from the BCS to BEC. In the BCS

*Email address: sgf02@mails.tsinghua.edu.cn

†Email address: hely04@mails.tsinghua.edu.cn

‡Email address: zhuangpf@mail.tsinghua.edu.cn

limit, the distribution near the Fermi surface is still very sharp and similar to the one in non-interacting fermion gas. However, it becomes very smooth in the whole momentum space in the BEC limit.

To be specific, we express the typical dispersion of fermion excitations in a superfluid as

$$E_{\mathbf{p}} = \sqrt{(\xi_{\mathbf{p}} - \mu)^2 + \Delta^2}, \quad (1)$$

where Δ is the superfluid order parameter. In non-relativistic homogeneous system, we have $\xi_{\mathbf{p}} = \mathbf{p}^2/(2m)$. In the BCS case, we have $\mu > 0$, the minimum of the dispersion is located at nonzero momentum $|\mathbf{p}| = \sqrt{2m\mu}$ and the excitation gap is Δ . However, when μ becomes negative in the BEC region, the excitation gap becomes $\sqrt{\mu^2 + \Delta^2}$ rather than Δ itself, and the minimum of the dispersion is located at $|\mathbf{p}| = 0$. This can be regarded as the definition of a BEC-BCS crossover at zero temperature. How can we extend this definition to relativistic systems? In relativistic case, we have $\xi_{\mathbf{p}} = \sqrt{\mathbf{p}^2 + m^2}$. In comparison with the non-relativistic result, we should define a new chemical potential $\mu_N = \mu - m$. For $\mu > m$, we have $\mu_N > 0$, the minimum of the dispersion is located at nonzero momentum $|\mathbf{p}| = \sqrt{\mu^2 - m^2}$ and the excitation gap is Δ . On the other hand, for $\mu < m$, μ_N becomes negative, the excitation gap becomes $\sqrt{\mu_N^2 + \Delta^2}$ and the minimum of the dispersion is located at $|\mathbf{p}| = 0$. This analysis indicates that the BEC-BCS crossover in relativistic fermion gas is controlled by $\mu_N = \mu - m$ rather than the chemical potential μ itself. An interesting phenomenon then arises: The BEC-BCS crossover would happen when the fermion mass m varies in the process of chiral symmetry restoration at finite temperature and density.

The effective models at hadron level can only describe the BEC state of bosons, they can not describe the possible BEC-BCS crossover when the chemical potential increases. One of the effective models that enables us to describe both quark and meson properties is the Nambu-Jona-Lasinio(NJL) model[49] applied to quarks[50, 51, 52, 53, 54]. Even though there is no confinement in the NJL model, the chiral phase transition line[50, 51, 52, 53, 54, 55, 56] in the temperature and baryon chemical potential $(T - \mu_B)$ plane calculated in the model is very close to the one obtained from lattice QCD. It is natural to extend the NJL model to studying diquark condensation at finite baryon chemical potential and pion condensation at finite isospin chemical potential. While there is no reliable lattice result for real QCD with diquark condensation at finite baryon chemical potential, the calculation of diquark condensation in the NJL model[28] agrees well with the lattice simulation of two color QCD[6, 7]. Also, the NJL model calculation of pion superfluidity[30] agrees well with the lattice simulation of real QCD at finite isospin chemical potential[10, 11, 12]. It is naturally to ask: How can such a model with quarks as elementary blocks describe the BEC-BCS crossover of diquarks and pions? In non-relativistic fermion gas, the microscopic model with

four-fermion interaction can describe well the BEC-BCS crossover at least at zero temperature[38, 41]. Motivated by this fact, we believe that the NJL model should describe well the BEC-BCS crossover in QCD at finite density.

The paper is organized as follows. In section II we investigate the diquark BEC-BCS crossover at finite baryon chemical potential in the NJL model of two color QCD. The possible diquark BEC-BCS crossover in real QCD is investigated in the NJL model in section III. In section IV we study the BEC-BCS crossover of pion condensation at finite isospin chemical potential. We summarize in section V.

II. DIQUARK BEC-BCS CROSSOVER IN TWO COLOR NJL MODEL

Let us first consider the diquark condensation in two color QCD. The advantage to take two color QCD is that the diquarks in this case are colorless baryons and the confinement is less important than in three color QCD. We start with the two color and two flavor NJL model[28]

$$\mathcal{L} = \bar{\psi}(i\gamma^\mu\partial_\mu - m_0)\psi + G_s \left[(\bar{\psi}\psi)^2 + (\bar{\psi}i\gamma_5\tau_5\psi)^2 \right] + G_d(\bar{\psi}i\gamma_5\tau_2t_2C\bar{\psi}^T)(\psi^T C i\gamma_5\tau_2t_2\psi), \quad (2)$$

where m_0 is the current quark mass, and τ_i and t_i are the Pauli matrices in flavor and color spaces. Since the couplings of the scalar meson and scalar diquark channels are the same, $G_s = G_d = G$, the enlarged flavor $SU(2N_f)$ symmetry of two color QCD is ensured, and the diquarks possess the same mass as the pions. The key quantity describing a thermodynamic system is the partition function Z which can be expressed as

$$Z = \int [d\bar{\psi}][d\psi] e^{\int_0^\beta d\tau \int d^3\mathbf{x} (\mathcal{L} + \frac{\mu_B}{2} \bar{\psi}\gamma_0\psi)} \quad (3)$$

in the imaginary time formalism of finite temperature field theory, where the baryon chemical potential μ_B is introduced explicitly, and β is the inverse temperature, $\beta = 1/T$. Using the Strotonovich-Hubbard transformation, we introduce the auxiliary meson fields σ, π and diquark field ϕ , and the partition function can be written as

$$Z = \int [d\bar{\Psi}][d\Psi][d\sigma][d\pi][d\phi][d\phi^*] e^{\int_0^\beta d\tau \int d^3\mathbf{x} \mathcal{L}_{\text{eff}}} \quad (4)$$

with the effective Lagrangian

$$\mathcal{L}_{\text{eff}} = \frac{1}{2} \bar{\Psi} \mathcal{K}[\sigma, \pi, \phi] \Psi - \frac{\sigma^2 + \pi^2 + |\phi|^2}{4G}, \quad (5)$$

where we have introduced the Nambu-Gorkov spinors

$$\Psi = \begin{pmatrix} \psi \\ C\bar{\psi}^T \end{pmatrix}, \quad \bar{\Psi} = (\bar{\psi} \ \psi^T C), \quad (6)$$

and the kernel \mathcal{K} is defined as

$$\mathcal{K}[\sigma, \pi, \phi] = \begin{pmatrix} \mathcal{M}_+ & i\gamma_5\phi\tau_2t_2 \\ i\gamma_5\phi^*\tau_2t_2 & \mathcal{M}_- \end{pmatrix} \quad (7)$$

with $\mathcal{M}_\pm = i\gamma^\mu\partial_\mu - m_0 \pm \mu_B\gamma_0/2 - (\sigma \pm i\gamma_5\tau \cdot \pi)$. Integrating out the quark degrees of freedom, we obtain

$$Z = \int [d\sigma][d\pi][d\phi][d\phi^*]e^{-S_{\text{eff}}[\sigma, \pi, \phi]} \quad (8)$$

with the bosonic effective action

$$S_{\text{eff}}[\sigma, \pi, \phi] = \int_0^\beta d\tau \int d^3\mathbf{x} \frac{\sigma^2 + \pi^2 + |\phi|^2}{4G} - \frac{1}{2} \text{Tr} \ln \mathcal{K}[\sigma, \pi, \phi]. \quad (9)$$

A. Diquark Fluctuation at $T > T_c$

The diquarks would be condensed when the baryon chemical potential μ_B is larger than their mass $m_d = m_\pi$. In this subsection we focus on the region above the critical temperature T_c where the diquark condensate vanishes.

After a field shift $\sigma \rightarrow \langle \sigma \rangle + \sigma$ with $\langle \sigma \rangle = -2G\langle \bar{\psi}\psi \rangle$, the effective action $S_{\text{eff}}^{(0)}$ at zeroth order in meson and diquark fields gives the mean field thermodynamic potential Ω ,

$$\Omega = \frac{1}{\beta V} S_{\text{eff}}^{(0)} = \frac{(m - m_0)^2}{4G} + \frac{1}{2\beta V} \ln \det \mathcal{S}^{-1}, \quad (10)$$

where $m = m_0 + \langle \sigma \rangle$ is the effective quark mass, and \mathcal{S} is the quark propagator at mean field level

$$\mathcal{S} = \left(\gamma^\mu \partial_\mu - m + \frac{\mu_B}{2} \gamma_0 \sigma_3 \right)^{-1} \quad (11)$$

with σ_i being the Pauli matrices in the Nambu-Gorkov space. The quadratic term of the effective action reads

$$S_{\text{eff}}^{(2)}[\sigma, \pi, \phi] = \int_0^\beta d\tau \int d^3\mathbf{x} \frac{\sigma^2 + \pi^2 + |\phi|^2}{4G} + \frac{1}{4} \text{Tr} \{ \mathcal{S} \Sigma[\sigma, \pi, \phi] \mathcal{S} \Sigma[\sigma, \pi, \phi] \}, \quad (12)$$

where Σ is defined as

$$\Sigma[\sigma, \pi, \phi] = \begin{pmatrix} \sigma + i\gamma_5\tau \cdot \pi & i\gamma_5\phi\tau_2t_2 \\ i\gamma_5\phi^*\tau_2t_2 & \sigma - i\gamma_5\tau \cdot \pi \end{pmatrix}. \quad (13)$$

In the momentum space, the second order effective action can be expressed as

$$S_{\text{eff}}^{(2)}[\sigma, \pi, \phi] = \frac{1}{2} \sum_k \left[\left[\frac{1}{2G} - \Pi_\sigma(k) \right] \sigma(-k)\sigma(k) + \left[\frac{1}{2G} - \Pi_\pi(k) \right] \pi(-k) \cdot \pi(k) + \left[\frac{1}{2G} - \Pi_d(k) \right] \phi^*(-k)\phi(k) + \left[\frac{1}{2G} - \Pi_{\bar{d}}(k) \right] \phi(-k)\phi^*(k) \right], \quad (14)$$

where $k = (k_0, \mathbf{k})$ with $k_0 = i\omega_n = 2in\pi T (n = 0, 1, 2, \dots)$ is the meson or diquark four momentum, and $\sum_k = iT \sum_n \int d^3\mathbf{k}/(2\pi)^3$ indicates integration over the three momentum \mathbf{k} and summation over the frequency ω_n . The polarization functions for the mesons, diquark and anti-diquark can be evaluated as

$$\begin{aligned} \Pi_\sigma(k) &= 2\Pi_1(k; \mu_B), & \Pi_\pi(k) &= 2\Pi_2(k; \mu_B), \\ \Pi_d(k) &= 2\Pi_3(k; \mu_B), & \Pi_{\bar{d}}(k) &= 2\Pi_4(k; \mu_B) \end{aligned} \quad (15)$$

with the functions $\Pi_{1,2,3,4}(k; \mu)$ listed in Appendix A.

Without loss of generality, we consider the case $\mu_B > 0$. The transition temperature T_c for the diquark condensation is determined by the well-known Thouless criterion

$$1 - 2G\Pi_d(k=0) \Big|_{T=T_c} = 0 \quad (16)$$

together with the gap equation for the effective quark mass derived from the first order derivative of the thermodynamic potential,

$$\frac{m - m_0}{16Gm} = \int \frac{d^3\mathbf{p}}{(2\pi)^3} \frac{1 - f(E_\mathbf{p}^+) - f(E_\mathbf{p}^-)}{E_\mathbf{p}} \Big|_{T=T_c} \quad (17)$$

with the particle energies $E_\mathbf{p} = \sqrt{\mathbf{p}^2 + m^2}$ and $E_\mathbf{p}^\pm = E_\mathbf{p} \pm \mu_B/2$.

Since the NJL model is non-renormalizable, we should employ a hard three momentum cutoff Λ to regularize the above equations. In the following numerical calculations, we take the current quark mass $m_0 = 5$ MeV, the coupling constant $G = 1.5 \times 4.93$ GeV $^{-2}$ and the cutoff $\Lambda = 653$ MeV to fit the pion mass $m_\pi = 134$ MeV, the pion decay constant $f_\pi = 93$ MeV and the constituent quark mass $m = 300$ MeV in the vacuum.

The critical temperature as a function of baryon chemical potential is shown in Fig.1. The diquark condensed phase starts at $\mu_B = m_\pi$ and the critical temperature increases with μ_B until a saturation value which is about the critical temperature for chiral symmetry restoration at $\mu_B = 0$, $T_0 = 185$ MeV. At moderate baryon chemical potential, the critical temperature can be well described by[57]

$$T_c = T_0 \sqrt{1 - \left(\frac{m_\pi}{\mu_B} \right)^4}. \quad (18)$$

We discuss now the mesons and diquarks above T_c . The energy dispersions of the mesons and diquarks are defined by the poles of their propagators,

$$1 - 2G\Pi_i(\omega(\mathbf{k}), \mathbf{k}) = 0, \quad i = \sigma, \pi, d, \bar{d}. \quad (19)$$

While the full dispersion laws can be obtained numerically, we are interested here only in the meson and diquark masses. For σ and π , they do not carry baryon number, and their masses are defined as $m_\sigma = \omega_\sigma(0)$ and $m_\pi = \omega_\pi(0)$. However, diquarks and anti-diquarks

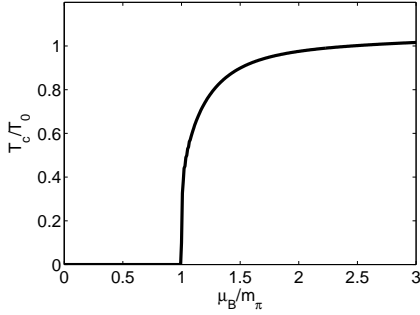


FIG. 1: The superfluid phase transition temperature T_c scaled by T_0 as a function of baryon chemical potential μ_B scaled by m_π .

carry baryon numbers and their masses are not exactly their dispersions at $\mathbf{k} = 0$. To define a proper diquark or anti-diquark mass, we should subtract the corresponding baryon chemical potential from the dispersion, $m_d = \omega_d(0) + \mu_B$ and $m_{\bar{d}} = \omega_{\bar{d}}(0) - \mu_B$. For $\mu_B > 0$, at the transition temperature T_c , the diquark mass is equal to the baryon chemical potential,

$$m_d(T_c) = \mu_B, \quad (20)$$

which is consistent with the physical picture of relativistic BEC in boson field theory. In Fig.2 we show the meson and diquark mass spectrum above the critical temperature for $\mu_B < m_\pi$ and $\mu_B > m_\pi$. For $\mu_B < m_\pi$, the meson mass spectrum is similar to the case at $\mu_B = 0$, but the diquark mass is slightly different from the anti-diquark mass at high temperature. For $\mu_B > m_\pi$, the mass spectrum starts at T_c where the diquark mass is exactly equal to μ_B . For any μ_B , we found that the meson or diquark mass becomes divergent at a limit temperature T^* which indicates the dissociation of the meson or diquark resonances. For small baryon chemical potential, this dissociation temperature is about two times the critical temperature for chiral symmetry restoration, which is consistent with the results in [58]. With increasing baryon chemical potential, while the dissociation temperature for diquarks and mesons decreases, the one for anti-diquarks increases. Since the diquarks are condensed at positive μ_B , the baryon chemical potential dependence of the diquark dissociation temperature indicates a crossover from diquark BEC to BCS superfluidity. In Fig.3, we show the superfluid transition temperature T_c and the dissociation temperature T^* for mesons, diquarks and anti-diquarks. Any T^* is much larger than T_c at small μ_B , but for mesons and diquarks the two temperatures tend to coincide with each other at sufficiently large μ_B .

To investigate the diquark excitation in detail, we consider the diquark spectral function

$$\rho(\omega, \mathbf{k}) = -2\text{Im}D_R(\omega, \mathbf{k}), \quad (21)$$

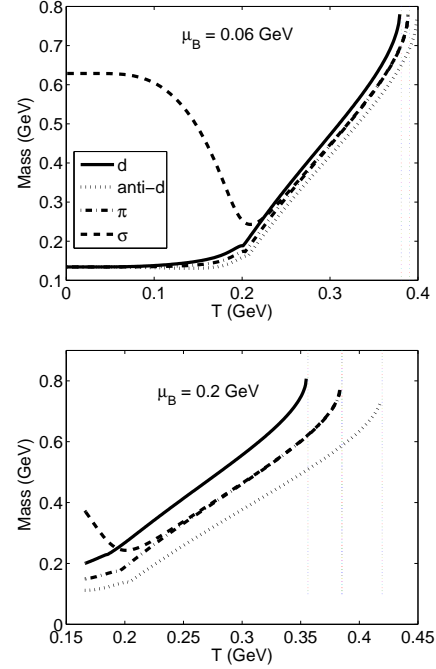


FIG. 2: The meson and diquark masses as functions of temperature for $\mu_B = 0.06$ GeV and 0.2 GeV.

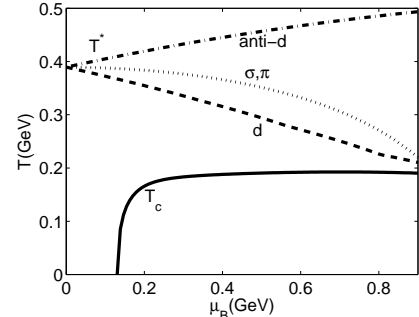


FIG. 3: The meson and diquark dissociation temperatures as functions of the baryon chemical potential.

where $D_R(\omega, \mathbf{k}) \equiv \mathcal{D}(\omega + i\eta, \mathbf{k})$ is the analytical continuation of the diquark Green function $\mathcal{D}(i\omega_n, \mathbf{k})$ defined as

$$\mathcal{D}(i\omega_n, \mathbf{k}) = \frac{2G}{1 - 2G\Pi_d(i\omega_n, \mathbf{k})}. \quad (22)$$

The spectral function ρ can be rewritten as

$$\begin{aligned} \rho(\omega, \mathbf{k}) = & \quad (23) \\ & -8G^2 \text{Im} \Pi_d(\omega + i\eta, \mathbf{k}) \\ & \frac{[1 - 2G\text{Re} \Pi_d(\omega + i\eta, \mathbf{k})]^2 + [2G\text{Im} \Pi_d(\omega + i\eta, \mathbf{k})]^2}{[1 - 2G\text{Re} \Pi_d(\omega + i\eta, \mathbf{k})]^2 + [2G\text{Im} \Pi_d(\omega + i\eta, \mathbf{k})]^2}. \end{aligned}$$

At zero momentum $\mathbf{k} = 0$, the real and imaginary parts

of the diquark polarization function can be evaluated as

$$\begin{aligned} \text{Re}\Pi_d(\omega + i\eta, \mathbf{0}) &= (24) \\ &- 8 \int \frac{d^3\mathbf{p}}{(2\pi)^3} \left[\frac{1 - 2f(E_{\mathbf{p}}^-)}{\omega - 2E_{\mathbf{p}} + \mu_B} - \frac{1 - 2f(E_{\mathbf{p}}^+)}{\omega + 2E_{\mathbf{p}} + \mu_B} \right], \\ \text{Im}\Pi_d(\omega + i\eta, \mathbf{0}) &= \\ &- 8\pi \int \frac{d^3\mathbf{p}}{(2\pi)^3} \left[(1 - 2f(E_{\mathbf{p}}^-))\delta(\omega - 2E_{\mathbf{p}} + \mu_B) \right. \\ &\quad \left. - (1 - 2f(E_{\mathbf{p}}^+))\delta(\omega + 2E_{\mathbf{p}} + \mu_B) \right] \\ &= \frac{2}{\pi} [p_{\omega} E_{p_{\omega}} (1 - 2f(E_{p_{\omega}}^-))] \Theta(\omega + \mu_B - 2m), \end{aligned}$$

with

$$p_{\omega} = \sqrt{\left(\frac{\omega + \mu_B}{2}\right)^2 - m^2}. \quad (25)$$

For $\mu_B < 2m$, a diquark can decay into two quarks only when its energy satisfies $\omega > 2m - \mu_B$, due to the step function Θ in the imaginary part. However, for $\mu_B > 2m$, a diquark can decay into two quarks at any energy and hence becomes an unstable resonance. In Fig.4 we show the diquark spectral function at zero momentum for several values of baryon chemical potential near the critical temperature T_c . For small baryon chemical potential $\mu_B < 2m$, the diquarks are in stable bound state at small energy $\omega < 2m - \mu_B$ and in unstable resonant state at large $\omega > 2m - \mu_B$. For large baryon chemical potential $\mu_B > 2m$, the diquarks are impossible to stay in bound state. With increasing baryon chemical potential, the diquarks become more and more unstable and finally disappear. This naturally supports the picture of diquark BEC-BCS crossover.

To understand more clearly the crossover from diquark BEC to BCS superfluidity, we come back to the BEC-BCS crossover in non-relativistic condensed matter physics. A signal of the crossover is that in the BEC region the chemical potential becomes negative and its absolute value tends to be half of the molecule binding energy. Therefore, the fermions are heavy and hard to be excited even at finite temperature, and only molecules survive and condense in the BEC region. In relativistic systems, we should subtract the fermion mass from the chemical potential in order to compare with the non-relativistic result. For this purpose, we define a new chemical potential

$$\mu_N = \frac{\mu_B}{2} - m. \quad (26)$$

In the deep BCS limit with $\mu_B \rightarrow \infty$, we have $m \rightarrow 0$ and $\mu_N \rightarrow \mu_B/2$, but in the deep BEC limit with $\mu_B \rightarrow m_{\pi}$, m tends to be its vacuum value, and μ_N becomes negative and its absolute value approaches to half of the diquark binding energy $\varepsilon_b = 2m - m_{\pi}$. In Fig.5 we show the effective quark mass m and the chemical potential μ_N at the critical temperature. The effective quark mass

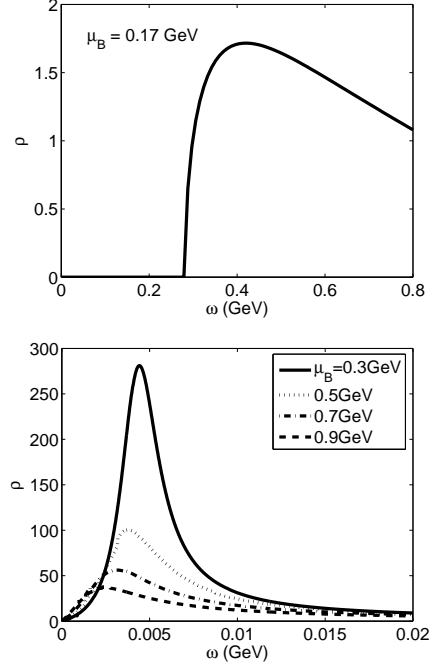


FIG. 4: The scaled diquark spectral function at zero momentum for small and large baryon chemical potentials.

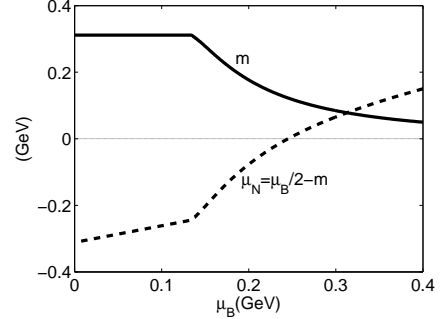


FIG. 5: The effective quark mass m and the corresponding chemical potential μ_N as functions of baryon chemical potential at the critical temperature.

decreases gradually from its vacuum value to zero with increasing baryon chemical potential. Since the lowest quark excitation energy is $\sqrt{\mathbf{p}^2 + m^2} - \mu_B/2$, the quarks are hard to be excited near the critical temperature if m is much larger than $\mu_B/2$. Obviously, at small μ_B , the diquarks are easy to be excited near T_c . This means that even though the elementary blocks of the NJL model are quarks, the true physical picture at small baryon chemical potential is the BEC of diquarks. The baryon chemical potential μ_B^0 corresponding to the crossover can be defined as $\mu_B = 2m$ which is just the point where the diquarks become unstable resonances. From Fig.5, μ_B^0 is about 240 MeV. We will give an analytical expression for

μ_B^0 in the next subsection.

B. Diquark Condensation at $T < T_c$

In this section we focus on the quark and diquark behavior in the superfluid phase. We start from the effective action (9). Since diquarks are condensed, we should introduce not only the chiral condensate $\langle\sigma\rangle$ but also the diquark condensates,

$$\langle\phi^*\rangle = \frac{\Delta}{\sqrt{2}}e^{i\theta}, \quad \langle\phi\rangle = \frac{\Delta}{\sqrt{2}}e^{-i\theta}. \quad (27)$$

A nonzero diquark condensate $\Delta \neq 0$ means spontaneous breaking of $U_B(1)$ baryon number symmetry in the two color QCD. The phase factor θ indicates the direction of the $U_B(1)$ symmetry breaking. For a homogeneous superfluid, we can choose $\theta = 0$ without loss of generality. A gapless Goldstone boson will appear, which can be identified as the quantum fluctuation in the phase direction. This Goldstone boson is just the Bogoliubov phonon in the superfluid.

After a field shift $\sigma \rightarrow \langle\sigma\rangle + \sigma$ and $\phi \rightarrow \Delta + \phi$, the effective action at zeroth order in meson and diquark fields gives the mean field thermodynamic potential

$$\Omega = \frac{1}{\beta V} S_{\text{eff}}^{(0)} = \frac{(m - m_0)^2 + \Delta^2}{4G} + \frac{1}{2\beta V} \ln \det \mathcal{S}_\Delta^{-1}, \quad (28)$$

where \mathcal{S}_Δ is the mean field quark propagator in the superfluid phase. In the momentum space it can be evaluated as

$$\mathcal{S}_\Delta(p) = \left(\gamma^\mu p_\mu - m + \frac{\mu_B}{2} \gamma_0 \sigma_3 + i\gamma_5 \Delta \tau_2 t_2 \sigma_1 \right)^{-1} \quad (29)$$

with the quark four momentum $p = (i\nu_n, \mathbf{p}) = ((2n+1)i\pi T, \mathbf{p})$ ($n = 0, 1, 2, \dots$). In the Nambu-Gorkov space, it can be explicitly expressed as a matrix

$$\mathcal{S}_\Delta(p) = \begin{pmatrix} \mathcal{S}_{11}(p) & \mathcal{S}_{12}(p) \\ \mathcal{S}_{21}(p) & \mathcal{S}_{22}(p) \end{pmatrix} \quad (30)$$

with the elements

$$\begin{aligned} \mathcal{S}_{11} &= \frac{(i\nu_n + E_\mathbf{p}^-) \Lambda_+ \gamma_0}{(i\nu_n)^2 - (E_\Delta^-)^2} + \frac{(i\nu_n - E_\mathbf{p}^+) \Lambda_- \gamma_0}{(i\nu_n)^2 - (E_\Delta^+)^2}, \\ \mathcal{S}_{22} &= \frac{(i\nu_n - E_\mathbf{p}^-) \Lambda_- \gamma_0}{(i\nu_n)^2 - (E_\Delta^-)^2} + \frac{(i\nu_n + E_\mathbf{p}^+) \Lambda_+ \gamma_0}{(i\nu_n)^2 - (E_\Delta^+)^2}, \\ \mathcal{S}_{12} &= \frac{-i\Delta \tau_2 t_2 \Lambda_+ \gamma_5}{(i\nu_n)^2 - (E_\Delta^-)^2} + \frac{-i\Delta \tau_2 t_2 \Lambda_- \gamma_5}{(i\nu_n)^2 - (E_\Delta^+)^2}, \\ \mathcal{S}_{21} &= \frac{-i\Delta \tau_2 t_2 \Lambda_- \gamma_5}{(i\nu_n)^2 - (E_\Delta^-)^2} + \frac{-i\Delta \tau_2 t_2 \Lambda_+ \gamma_5}{(i\nu_n)^2 - (E_\Delta^+)^2}, \end{aligned} \quad (31)$$

where Λ_\pm are the energy projectors

$$\Lambda_\pm(\mathbf{p}) = \frac{1}{2} \left[1 \pm \frac{\gamma_0 (\vec{\gamma} \cdot \mathbf{p} + m)}{E_\mathbf{p}} \right], \quad (32)$$

and $E_\Delta^\pm = \sqrt{(E_\mathbf{p}^\pm)^2 + \Delta^2}$ are quark energies in the superfluid phase. The momentum distributions of quarks and anti-quarks can be calculated from the positive and negative energy components of the diagonal propagators \mathcal{S}_{11} and \mathcal{S}_{22} ,

$$\begin{aligned} n_q(\mathbf{p}) &= \sum_n \frac{i\nu_n + E_\mathbf{p}^-}{(i\nu_n)^2 - (E_\Delta^-)^2} e^{i\nu_n \eta} = \frac{1}{2} \left(1 - \frac{E_\mathbf{p}^-}{E_\Delta^-} \right), \\ n_{\bar{q}}(\mathbf{p}) &= \sum_n \frac{i\nu_n + E_\mathbf{p}^+}{(i\nu_n)^2 - (E_\Delta^+)^2} e^{i\nu_n \eta} = \frac{1}{2} \left(1 - \frac{E_\mathbf{p}^+}{E_\Delta^+} \right). \end{aligned} \quad (33)$$

It has been demonstrated in non-relativistic models that the BCS mean field theory can describe well the BEC-BCS crossover at low temperature, $T \ll T_c$. Here we will treat the ground state in the mean field approximation. The gap equations to determine the effective quark mass m and diquark condensate Δ can be obtained by the minimum of the thermodynamic potential,

$$\frac{\partial \Omega}{\partial m} = 0, \quad \frac{\partial \Omega}{\partial \Delta} = 0. \quad (34)$$

With the explicit form of the thermodynamic potential

$$\Omega = \frac{(m - m_0)^2 + \Delta^2}{4G} - 8 \int \frac{d^3 \mathbf{p}}{(2\pi)^3} [\zeta(E_\Delta^+) + \zeta(E_\Delta^-)], \quad (35)$$

where ζ is defined as $\zeta(x) = x/2 + \beta^{-1} \ln(1 + e^{-\beta x})$, we obtain the gap equations at zero temperature

$$\begin{aligned} m - m_0 &= 8Gm \int \frac{d^3 \mathbf{p}}{(2\pi)^3} \frac{1}{E_\mathbf{p}} \left(\frac{E_\mathbf{p}^-}{E_\Delta^-} + \frac{E_\mathbf{p}^+}{E_\Delta^+} \right), \\ \Delta &= 8G\Delta \int \frac{d^3 \mathbf{p}}{(2\pi)^3} \left(\frac{1}{E_\Delta^-} + \frac{1}{E_\Delta^+} \right). \end{aligned} \quad (36)$$

Numerical solution of the gap equations is shown in Fig.6. Our results for the chiral and diquark condensates agree quite well with the lattice data[28]. For $\mu_B < m_\pi$ the ground state is the same as the vacuum state and the baryon density keeps zero. For $\mu_B > m_\pi$ the diquark condensate and baryon density become nonzero. The critical baryon chemical potential μ_B^c is exactly the diquark mass m_d in the vacuum, and the phase transition is of second order. Since the chiral symmetry is spontaneously broken at small μ_B and almost restored at large μ_B , the effective quark mass m plays an important role at small μ_B but can be neglected at large μ_B . In fact, in the region above but close to the critical value μ_B^c , the chiral condensate, effective quark mass and the diquark condensate as functions of μ_B can be well described by[30]

$$\begin{aligned} \frac{m(\mu_B)}{m(0)} &\simeq \frac{\langle\sigma\rangle(\mu_B)}{\langle\sigma\rangle(0)} = \left(\frac{m_\pi}{\mu_B} \right)^2, \\ \frac{\Delta(\mu_B)}{\langle\sigma\rangle(0)} &= \sqrt{1 - \left(\frac{m_\pi}{\mu_B} \right)^4}, \end{aligned} \quad (37)$$

which are consistent with the results from the chiral effective theory[14].

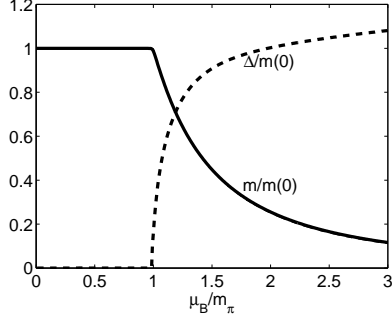


FIG. 6: The diquark condensate and the effective quark mass scaled by the quark mass in the vacuum as functions of μ_B/m_π at zero temperature.

To explain the BEC-BCS crossover, we further consider the dispersions of quark excitations,

$$E_\Delta^\pm = \sqrt{\left(\sqrt{\mathbf{p}^2 + m^2} \pm \mu_B/2\right)^2 + \Delta^2}. \quad (38)$$

In the case of $\mu_B > 0$, E_Δ^+ is the anti-particle excitation. In Fig.7 we show the dispersion E_Δ^- at $\mu_B = 0.15, 0.5, 0.9$ GeV. Obviously, the fermion excitations are always gapped. At small μ_B with $\mu_B/2 < m(\mu_B)$, the minimum of the dispersion is at $|\mathbf{p}| = 0$ where the energy gap is $\sqrt{\mu_N^2 + \Delta^2}$ with the corresponding non-relativistic chemical potential $\mu_N = \mu_B/2 - m$ introduced in the last subsection. However, at large μ_B with $\mu_B/2 > m(\mu_B)$, the minimum of the dispersion is shifted to $|\mathbf{p}| \simeq \mu_B/2$ where the energy gap is Δ . Such a phenomenon is a signal of the BEC-BCS crossover.

The BEC-BCS crossover is also reflected in the momentum dependence of the quark occupation number. In Fig.7 we show also the quark momentum distribution $n_q(\mathbf{p})$ at $\mu_B = 0.15, 0.5, 0.9$ GeV. At small μ_B such as $\mu_B = 0.15$ GeV the occupation number is very small and smooth in the whole momentum region, while at large μ_B the occupation number becomes large near $|\mathbf{p}| = 0$ and drops down with increasing momentum rapidly. When μ_B becomes very large, the occupation number is indeed of the BCS type.

The numerical results of the chemical potential μ_N is shown in Fig.8. The turning point from negative μ_N to positive μ_N is at about $\mu_B^0 \simeq 230$ MeV, which is nearly the same as we obtained at the critical temperature shown in the last subsection. In fact, we can get an analytical expression for μ_B^0 using equation (37). The BEC region is obtained by requiring $\mu_N < 0$, namely

$$\frac{\mu_B}{2} < m(\mu_B) = m(0) \left(\frac{m_\pi}{\mu_B}\right)^2, \quad (39)$$

from which we obtain

$$\mu_B^0 = [2m(0)m_\pi^2]^{1/3}, \quad (40)$$

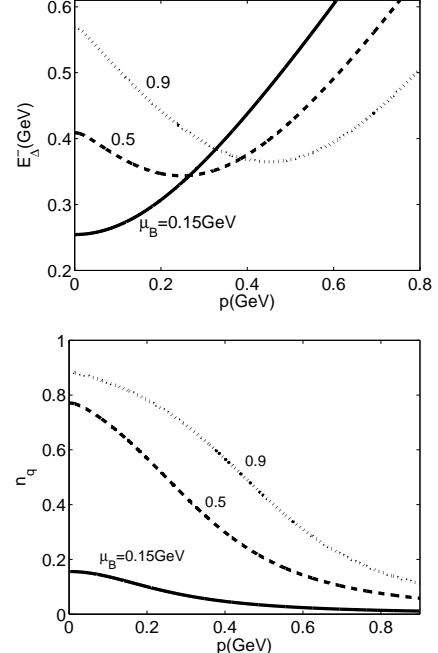


FIG. 7: The quark energy dispersion and momentum distribution at several baryon chemical potentials at zero temperature.

it depends on the pion mass and effective quark mass in the vacuum. With the above chosen parameter set, we have $\mu_B^0 = 230$ MeV. When the effective quark mass in the vacuum varies from 300 MeV to 500 MeV, μ_B^0 changes from 230 MeV to 270 MeV. Note that the explicit chiral symmetry breaking induced by nonzero current quark mass m_0 plays an important role in the study of BEC-BCS crossover. In the chiral limit with $m_0 = 0$, pions are massless and there will be no BEC state.

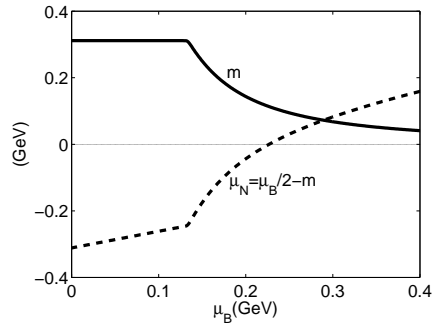


FIG. 8: The effective quark mass and non-relativistic chemical potential μ_N as functions of baryon chemical potential at zero temperature.

We now turn to the meson and diquark excitations. The second order effective action which is quadratic in

the meson and diquark fields can be expressed as

$$S_{\text{eff}}^{(2)}[\sigma, \pi, \phi] = \int_0^\beta d\tau \int d^3\mathbf{x} \frac{\sigma^2 + \pi^2 + |\phi|^2}{4G} + \frac{1}{4} \text{Tr} \{ \mathcal{S}_\Delta \Sigma[\sigma, \pi, \phi] \mathcal{S}_\Delta \Sigma[\sigma, \pi, \phi] \}, \quad (41)$$

and can be evaluated as

$$S_{\text{eff}}^{(2)}[\sigma, \pi, \phi] = \frac{1}{2} \sum_k \left[\frac{\delta_{ij}}{2G} - \Pi_{ij}(k) \right] \varphi_i(-k) \varphi_j(k) \quad (42)$$

in the momentum space, where φ_i stand for the meson and diquark fields σ, π, ϕ and ϕ^* , and the polarization functions Π_{ij} are defined as

$$\Pi_{ij}(k) = i \int \frac{d^4p}{(2\pi)^4} \text{Tr} [\Gamma_i \mathcal{S}_\Delta(p+k) \Gamma_j \mathcal{S}_\Delta(p)] \quad (43)$$

with Γ_i being the interaction vertex defined in the Lagrangian density (2).

Due to the off-diagonal elements of the quark propagator (30), those eigen modes of the system above T_c are, in general case, no longer the eigen modes of the Hamiltonian in the superfluid phase. The new eigen modes are linear combinations of the old eigen modes and their masses are controlled by the determinant of the meson and diquark polarizations

$$\det \left[\frac{\delta_{ij}}{2G} - \Pi_{ij}(k_0 = M, \mathbf{k} = 0) \right] = 0. \quad (44)$$

It can be analytically proven that while pions do not mix with the others and hence are still the eigen modes of the system, there is indeed a mixing among sigma, diquark and anti-diquark[28], and this mixing leads to a gapless Goldstone boson. We can show that $\Pi_{\sigma d}$ and $\Pi_{\sigma \bar{d}}$ are proportional to $m\Delta$ and $\Pi_{d\bar{d}}$ is proportional to Δ^2 . Therefore, the mixing between sigma and diquark or anti-diquark is very strong in the BEC region where m and Δ coexist and are both large, but the mixing can be neglected at large baryon chemical potential where m approaches to zero.

C. Phase Diagram in $T - \mu_B$ Plane

We can now summarize the above results and propose a phase diagram of two color QCD in the $T - \mu_B$ plane. The phase diagram is shown in Fig.9. At low temperature and low baryon chemical potential, the matter should be in the normal hadron state. The thick dashed line at high temperature means the estimated phase transition from hadron gas to quark gas, which can not be calculated in the NJL model but should exist in the system. When the baryon chemical potential becomes larger than the pion mass in the vacuum, the diquark BEC appears and exists up to another critical baryon chemical potential μ_B^0 indicated by the vertical dashed line. At high enough baryon

chemical potential, the matter will become the BCS superfluid where the quark-quark Cooper pairs are condensed. Between the BEC and BCS states there should exist a crossover region, like the pseudogap regime in high temperature superconductor and ultracold fermion gas. Since two color QCD can be successfully simulated on lattice, such a BEC-BCS crossover can be confirmed by measuring the quark energy gap and comparing it with the diquark condensate. The pseudogap phase at high temperature can also be confirmed by investigating the quark spectral function.

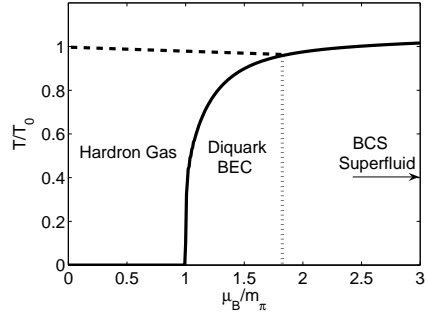


FIG. 9: The proposed phase diagram of diquark condensation in two color QCD in the $T - \mu_B$ plane.

III. DIQUARK BEC-BCS CROSSOVER IN THREE COLOR NJL MODEL

Let us now consider the realistic world with color degrees of freedom $N_c = 3$. The three color NJL model including the scalar diquark channel is defined as

$$\mathcal{L} = \bar{\psi} (i\gamma^\mu \partial_\mu - m_0) \psi + G_s \left[(\bar{\psi} \psi)^2 + (\bar{\psi} i\gamma_5 \tau \psi)^2 \right] + G_d \sum_{a=2,5,7} (\bar{\psi} i\gamma^5 \tau_2 \lambda_a C \bar{\psi}^T) (\psi^T C i\gamma^5 \tau_2 \lambda_a \psi), \quad (45)$$

where λ_a are the Gell-Mann matrices in color space. Different from two color QCD, the scalar diquarks in three color case are color anti-triplets. Therefore, in real QCD, the problem of confinement becomes important. In this section, we will discuss the possible diquark BEC-BCS crossover without considering the effect of confinement.

A. Scalar Diquark Mass in the Vacuum

We first discuss the scalar diquark mass in the vacuum with $T = \mu_B = 0$. In the random phase approximation, the diquark mass is determined by the pole equation

$$1 - 2G_d \Pi_d(k_0 = m_d, \mathbf{k} = 0) = 0, \quad (46)$$

where the diquark polarization function is defined as

$$\Pi_d(k) = 4i \int \frac{d^4 p}{(2\pi)^4} \text{Tr} [i\gamma_5 \mathcal{S}(p+k) i\gamma_5 \mathcal{S}(p)] \quad (47)$$

with the mean field quark propagator $\mathcal{S}(p) = (\gamma^\mu p_\mu - m)^{-1}$. The effective quark mass m defined as $m = m_0 - 2G_s \langle \bar{\psi} \psi \rangle$ satisfies the gap equation

$$m - m_0 = 24G_s m \int \frac{d^3 \mathbf{p}}{(2\pi)^3} \frac{1}{\sqrt{\mathbf{p}^2 + m^2}}. \quad (48)$$

Taking the trace in the Dirac space and summation over the quark frequency, the diquark mass m_d is controlled by

$$1 = 8G_d \int \frac{d^3 \mathbf{p}}{(2\pi)^3} \left(\frac{1}{E_{\mathbf{p}} + m_d/2} + \frac{1}{E_{\mathbf{p}} - m_d/2} \right). \quad (49)$$

Since diquarks can not exist as stable bound states in the vacuum, their mass must satisfy the constraint $0 < m_d < 2m$. As a consequence, the coupling constant in the scalar diquark channel should be in the region $G_d^{\min} < G_d < G_d^{\max}$ [59, 60], where the up limit is nearly model independent,

$$G_d^{\max} = \frac{3}{2} G_s \frac{m}{m - m_0} \simeq \frac{3}{2} G_s, \quad (50)$$

but the low limit depends on the model parameters,

$$G_d^{\min} = \frac{\pi^2}{4 \left(\Lambda \sqrt{\Lambda^2 + m^2} + m^2 \ln \frac{\Lambda + \sqrt{\Lambda^2 + m^2}}{m} \right)}. \quad (51)$$

In the three color NJL model, the model parameters are set to be $m_0 = 5$ MeV, $G_s = 4.93$ GeV $^{-2}$ and $\Lambda = 653$ MeV. For convenience, we take the coupling ratio $\eta = G_d/G_s$ instead of G_d . With the above parameter values, we find $\eta_{\max} \simeq 1.55$ and $\eta_{\min} \simeq 0.82$. For other possible parameter values, the low limit is roughly in the region $0.7 < \eta_{\text{extmin}} < 0.8$. Physically speaking, if $\eta > \eta_{\max}$, the vacuum becomes unstable, and if $\eta < \eta_{\min}$, a scalar diquark can decay into two quarks and becomes a unstable resonance.

The η dependence of the scalar diquark mass is shown in Fig.10. As estimated in [3], a scalar diquark is in a deeply bound state when the binding energy is in the region 200 MeV $< 2m - m_d < 300$ MeV, which corresponds to the diquark mass 300 MeV $< m_d < 400$ MeV and to the coupling ratio $1.3 < \eta < 1.4$.

B. Diquark BEC-BCS crossover

At large enough baryon chemical potential, the diquarks will condense. The diquark condensate is defined as

$$\Delta_a = -2G_d \langle \psi^T C i\gamma^5 \tau_2 \lambda_a \psi \rangle. \quad (52)$$

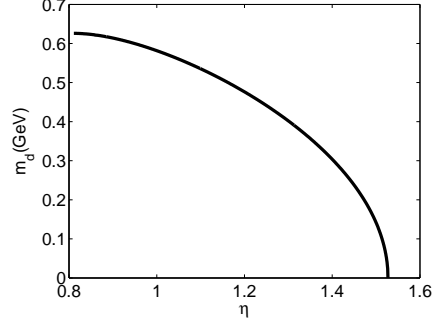


FIG. 10: The scalar diquark mass m_d in the vacuum as a function of the coupling ratio $\eta = G_d/G_s$.

Due to the color SU(3) symmetry, we can choose a specific gauge $\Delta_2 = \Delta \neq 0, \Delta_5 = \Delta_7 = 0$. In this gauge, the red and green quarks participate in the condensation, but the blue one does not. The thermodynamic potential at mean field level reads[61]

$$\begin{aligned} \Omega = & \frac{(m - m_0)^2}{4G_s} + \frac{\Delta^2}{4G_d} \\ & - 4 \int \frac{d^3 \mathbf{p}}{(2\pi)^3} [2(\zeta(E_{\Delta}^+) + \zeta(E_{\Delta}^-)) + \zeta(E_b^+) + \zeta(E_b^-)], \end{aligned} \quad (53)$$

where the quark energies are defined as

$$\begin{aligned} E_{\Delta}^{\pm} &= \sqrt{(E_{\mathbf{p}} \pm \mu_B/3)^2 + \Delta^2}, \\ E_b^{\pm} &= E_{\mathbf{p}} \pm \mu_B/3 \end{aligned} \quad (54)$$

with chemical potentials $\mu_r = \mu_g = \mu_b = \mu_B/3$ for the red, green and blue quarks. Minimizing the thermodynamic potential, we obtain the gap equations for the chiral and color condensates m and Δ at zero temperature,

$$\begin{aligned} m - m_0 &= 8G_s m \int \frac{d^3 \mathbf{p}}{(2\pi)^3} \frac{1}{E_{\mathbf{p}}} \left[\frac{E_{\mathbf{p}}^-}{E_{\Delta}^-} + \frac{E_{\mathbf{p}}^+}{E_{\Delta}^+} + \Theta(E_b^-) \right], \\ \Delta &= 8G_d \Delta \int \frac{d^3 \mathbf{p}}{(2\pi)^3} \left(\frac{1}{E_{\Delta}^-} + \frac{1}{E_{\Delta}^+} \right). \end{aligned} \quad (55)$$

The above gap equations are almost the same as in the two color case, except the term $\Theta(E_b^-)$ in the first equation. For $\eta < \eta_{\min}$, the diquark condensation takes place at about $\mu_B^c \simeq 3m$ and the phase transition is of first order. In this case, there exists no BEC region where $\mu_N \equiv \mu_r - m = \mu_B/3 - m$ is negative. On the other hand, For $\eta_{\min} < \eta < \eta_{\max}$, the diquarks become condensed at $\mu_B^c = 3m_d/2$ and the phase transition is of second order. The proof is as follows. For $\mu_B < 3m_d/2 < 3m$, the gap equation for m keeps the same form as in the vacuum, and the gap equation for Δ becomes

$$1 = 8G_d \int \frac{d^3 \mathbf{p}}{(2\pi)^3} \left(\frac{1}{E_{\mathbf{p}} + \mu_B^c/3} + \frac{1}{E_{\mathbf{p}} - \mu_B^c/3} \right) \quad (56)$$

at the phase transition of color superconductivity with $\Delta = 0$. From the comparison with the diquark mass equation in the vacuum, the critical baryon chemical potential for color superconductivity should be $\mu_B^c = 3m_d/2$ [60]. In this case, there must exist a BEC region where μ_N is negative, since at the phase transition point we have $\mu_N = \mu_B^c/3 - m = m_d/2 - m < 0$.

In Fig.11, we show the effective quark mass and diquark condensate as functions of baryon chemical potential. From the behavior of μ_N , there exists indeed a diquark BEC region at intermediate baryon chemical potential. At sufficiently large baryon chemical potential the diquark condensate is in the BCS form.

In the diquark BEC region, we assume that the effective quark mass behaves as

$$\frac{m(\mu_B)}{m(0)} \simeq \left(\frac{\mu_B^c}{\mu_B} \right)^\alpha, \quad \alpha > 0. \quad (57)$$

From our numerical calculation, the value of α depends on the coupling η . Taking $m(\mu_B) = \mu_B/3$ from $\mu_N = 0$ at the end point of the BEC, the diquark BEC region ends at

$$\mu_B^0 = \frac{3}{2} [2m(0)m_d^\alpha]^{1/\alpha+1}. \quad (58)$$

Therefore, the interval of μ_B for diquark BEC is

$$\Delta\mu_B = \mu_B^0 - \mu_B^c = \frac{3}{2}m_d \left[\left(\frac{2m(0)}{m_d} \right)^{1/\alpha+1} - 1 \right]. \quad (59)$$

The largest BEC region takes place at $m_d \simeq 185$ MeV corresponding to $\eta \simeq 1.46$.

The critical temperature T_c can be determined by solving the gap equations with $\Delta = 0$. Above the critical temperature, all scalar diquarks become degenerated and their polarization function reads $\Pi_d(k) = \Pi_3(k; 2\mu_B/3)$ with Π_3 listed in Appendix A. Similar to the calculation in the two color case, the diuarks are in bound state in the BEC region with $\mu_B/3 < m$, and become unstable resonances in the BCS region. The numerical results and discussions are quite similar to that in the two color NJL model.

C. Effect of Color Neutrality

In three color QCD, diquarks are no longer colorless and the requirement of color neutrality is not automatically satisfied once diquarks are included. This can be seen if we compute the expectation values of the color charges $\langle Q_a \rangle = \langle \bar{\psi} \lambda_a \gamma_0 \psi \rangle$. In the gauge with $\Delta_2 \neq 0$ and $\Delta_5 = \Delta_7 = 0$, we find $\langle Q_8 \rangle \neq 0$. To solve this problem, we can introduce a color chemical potential μ_8 corresponding to the 8-th color charge. It may be dynamically generated by a gluon condensate $\langle A_8^0 \rangle$. The color chemical potential enters the gap equations by replacing the quark chemical potentials $\mu_r = \mu_g = \mu_b = \mu_B/3$

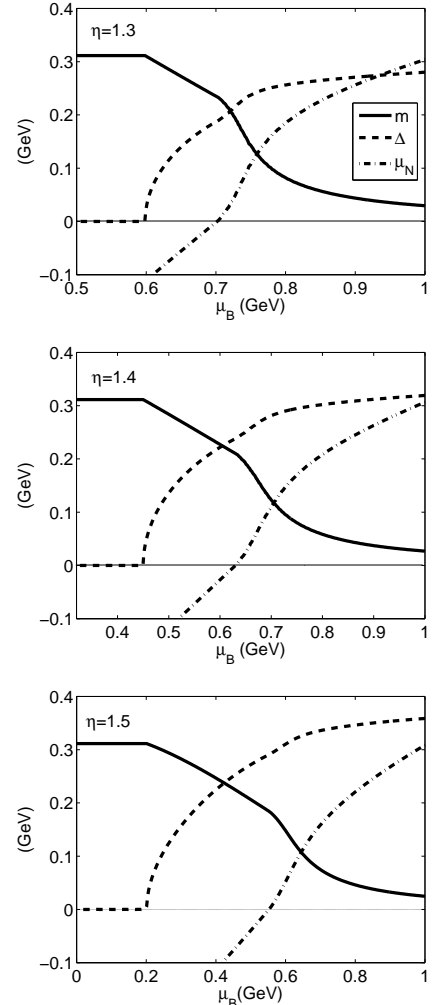


FIG. 11: The diquark condensate Δ , effective quark mass m and the chemical potential μ_N as functions of baryon chemical potential for several values of the coupling ratio η at zero temperature. The color neutrality is not taken into account.

by $\mu_r = \mu_g = \mu_B/3 + \mu_8/3$ and $\mu_b = \mu_B/3 - 2\mu_8/3$. The color charge neutrality condition is guaranteed by $n_8 = -\partial\Omega/\partial\mu_8 = 0$, namely

$$\int \frac{d^3\mathbf{p}}{(2\pi)^3} \left[\frac{E_{\mathbf{p}}^+}{E_\Delta^+} - \frac{E_{\mathbf{p}}^-}{E_\Delta^-} - 2\Theta(-E_b^-) \right] = 0. \quad (60)$$

Taking into account the color neutrality, the recalculated effective quark mass and diquark condensate are shown in Fig.12. Comparing the behavior of the effective chemical potential $\mu_N \equiv \mu_r - m$ in the two cases with and without considering color neutrality, we find that the requirement of color neutrality disfavors diquark BEC. However, it does not cancel the BEC region completely.

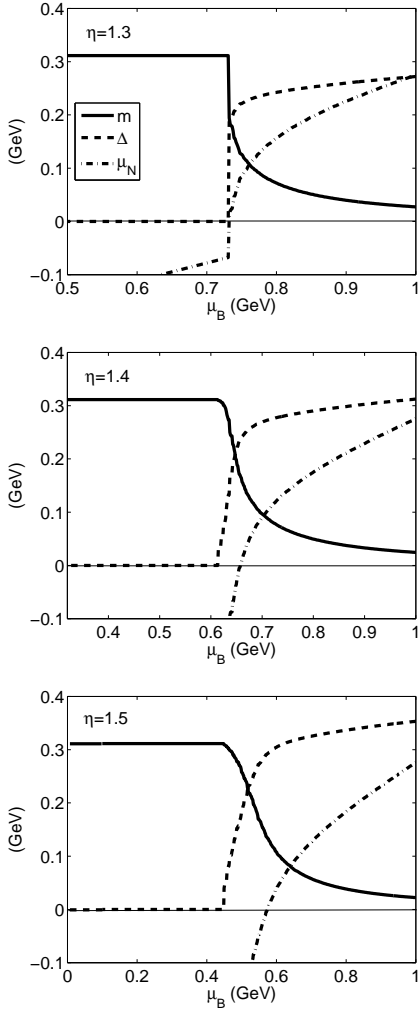


FIG. 12: The diquark condensate Δ , effective quark mass m and the chemical potential μ_N as functions of baryon chemical potential for several values of the coupling ratio η at zero temperature. The color neutrality is considered.

D. Effect of Vector Meson Coupling

Now we ask the question whether there exists some mechanism that favors the diquark BEC. As we have seen, the diquark BEC happens in the beginning part of color superconductivity where the broken chiral symmetry starts to restore and the effective quark mass is still large enough. As proposed in [62], the quark interaction in vector meson channel may be a candidate to slow down the chiral symmetry restoration and enhance the BEC formation. Now we include a new interaction term to the NJL lagrangian,

$$\mathcal{L}_v = -G_v \left[(\bar{\psi} \gamma_\mu \psi)^2 + (\bar{\psi} \gamma_\mu \gamma_5 \tau \psi)^2 \right], \quad (61)$$

which corresponds to vector mesons. At finite density, a new condensate $\rho_v = 2G_v \langle \bar{\psi} \gamma_0 \psi \rangle$ which is proportional

to the baryon number density should be considered. This condensate induces a new energy term $-\rho_v^2/4G_v$ in the thermodynamic potential and it enters the gap equations by replacing $\mu_B/3$ by $\mu_B/3 - \rho_v$. The gap equation for ρ_v at zero temperature reads

$$\rho_v = 8G_v \int \frac{d^3 \mathbf{p}}{(2\pi)^3} \left[\frac{E_\mathbf{p}^+}{E_\Delta^+} - \frac{E_\mathbf{p}^-}{E_\Delta^-} + \Theta(-E_b^-) \right]. \quad (62)$$

In Fig.13 we calculate the effective quark mass and the diquark condensate at the coupling ratio $\eta = 1$ and for three values of the vector coupling G_v . For $G_v = 0$ the diquark BEC region is almost not visible, but for a reasonably large vector coupling such as $G_v/G_s = 0.3$ or 0.5, there appears a large diquark BEC region. It is clear that the vector meson channel really slows down the chiral symmetry restoration and favors the formation of diquark BEC. There may exist other mechanisms that favor BEC, such as the axial anomaly in QCD[63].

E. Chromomagnetic Instability

For realistic QCD matter in nature such as in compact stars, beta equilibrium and charge neutrality should be considered. These effects induce a chemical potential mismatch $\delta\mu$ between u and d quarks. Assuming the ground state to be a uniform phase, the mismatch effect will lead to an interesting gapless color superconductivity phases[64, 65]. However, it was found that the gapless phase in the weak coupling region suffers the so-called chromomagnetic instability[66]: The Meissner masses squared of some gluons are negative. While the chromomagnetic instability indicates that the ground state of the superfluid may favor to be in some non-uniform phase such as LOFF phase[67, 68, 69], the instability may be cured in some region. Based on a two species model[70], it is found that the magnetic instability should be fully cured in the BEC region. However, the 4-7th gluons' instability is not yet examined. Here we try to complete this work.

The analytical expressions of the Meissner masses squared m_4^2 for the 4-7th gluons and m_8^2 for the 8th gluon are listed in Appendix B. We show the Meissner masses squared in Fig.14 in both BCS and BEC states. In the BCS case with $m \ll \mu_r$, our result is consistent with the analytical expression[66]. When we approach to the BEC region, both the 4-7th and 8th gluons' instabilities are partially cured. In the BEC region with $m \geq \mu_r$, they are fully cured. Our investigation here is consistent with the study based on a non-relativistic model[71]. Since the chromomagnetic instability is fully cured, the ground state in the BEC region should be a uniform phase. We should address that such a phenomenon is quite similar to what happens in non-relativistic systems[72, 73, 74].

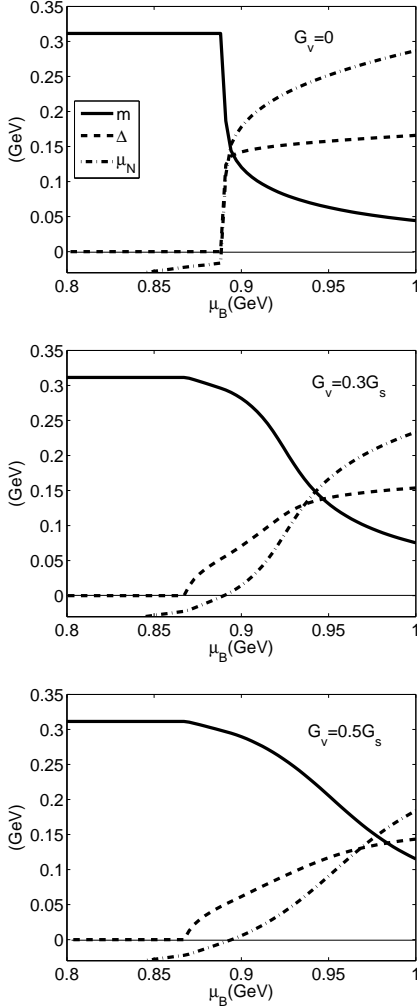


FIG. 13: The diquark condensate Δ , effective quark mass m and the chemical potential μ_N as functions of baryon chemical potential for several values of the vector couplings G_v and at a fixed diquark coupling ratio $\eta = 1$ at zero temperature.

IV. PION BEC-BCS CROSSOVER AT FINITE ISOSPIN DENSITY

Another BEC-BCS crossover in dense QCD happens at finite isospin density where pions become condensed[4]. At small isospin density, the QCD matter is a BEC of charged pions, but at ultra high isospin density, deconfinement happens and the matter turns to be a BCS superfluid with quark-antiquark cooper pairing[4]. Therefore, there should be a BEC to BCS crossover when the isospin chemical potential increases. From the similarity between pions in three color QCD and diquarks in two color QCD, the pion superfluidity discussed in this section is quite similar to the diquark superfluid in Section II. We start from the two flavor Nambu–Jona-Lasinio

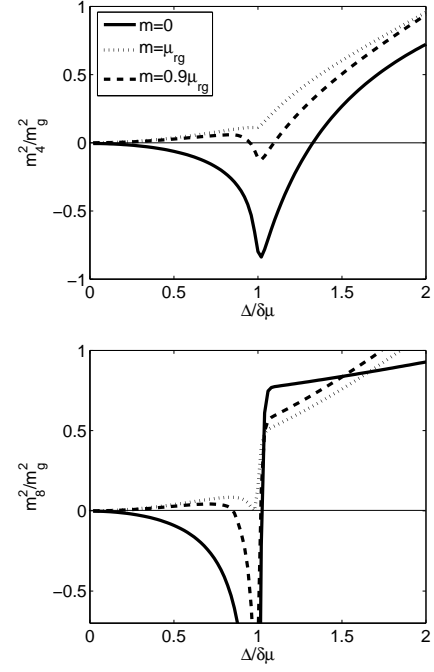


FIG. 14: The Meissner masses squared, scaled by $m_g^2 = 4\alpha_s\mu_r^2/(3\pi)$ with α_s being the QCD gauge coupling constant, for the 4-7th gluons (upper panel) and 8th gluon (lower panel) as functions of $\Delta/\delta\mu$.

model with only scalar meson channel,

$$\mathcal{L} = \bar{\psi} (i\gamma^\mu \partial_\mu - m_0) \psi + G_s \left[(\bar{\psi}\psi)^2 + (\bar{\psi}i\gamma_5\tau\psi)^2 \right]. \quad (63)$$

The key quantity describing the system is the partition function

$$Z = \int [d\bar{\psi}] [d\psi] e^{\int_0^\beta d\tau \int d^3\mathbf{x} [\mathcal{L} + \frac{\mu_I}{2} \bar{\psi}\gamma_0\tau_3\psi]}, \quad (64)$$

where the isospin chemical potential μ_I corresponds to the third component I_3 of the isospin charge. Using the Strotonovich-Hubbard transformation we introduce the auxiliary meson fields σ and π , and the partition function can be written as

$$Z = \int [d\bar{\psi}] [d\psi] [d\sigma] [d\pi] e^{\int_0^\beta d\tau \int d^3\mathbf{x} \mathcal{L}_{\text{eff}}} \quad (65)$$

with the effective Lagrangian

$$\mathcal{L}_{\text{eff}} = \bar{\psi} \mathcal{K}[\sigma, \pi] \psi - \frac{\sigma^2 + \pi^2}{4G_s} \quad (66)$$

where the kernel \mathcal{K} is defined as

$$\mathcal{K}[\sigma, \pi] = i\gamma^\mu \partial_\mu - m_0 + \frac{\mu_I}{2} \gamma_0 \tau_3 - (\sigma + i\gamma_5 \tau \cdot \pi). \quad (67)$$

Integrating out the quark degrees of freedom, we obtain

$$Z = \int [d\sigma] [d\pi] e^{-S_{\text{eff}}[\sigma, \pi]} \quad (68)$$

with the meson effective action

$$S_{\text{eff}}[\sigma, \pi] = \int_0^\beta d\tau \int d^3\mathbf{x} \frac{\sigma^2 + \pi^2}{4G_s} - \text{Tr} \ln \mathcal{K}[\sigma, \pi]. \quad (69)$$

A. Pion Fluctuation at $T > T_c$

As we expected, when the isospin chemical potential μ_I becomes larger than the pion mass m_π in the vacuum, the charged pions will condense at low temperature. In this subsection we focus on the region above the critical temperature T_c where pion condensate vanishes. After the field shift for σ , the effective action at zeroth order in meson fields gives the mean field thermodynamic potential Ω ,

$$\Omega = \frac{1}{\beta V} S_{\text{eff}}^{(0)} = \frac{(m - m_0)^2}{4G_s} + \frac{1}{\beta V} \ln \det \mathcal{S}^{-1}, \quad (70)$$

where \mathcal{S} is the quark propagator at mean field level

$$\mathcal{S} = \left(\gamma^\mu \partial_\mu - m + \frac{\mu_I}{2} \gamma_0 \tau_3 \right)^{-1}. \quad (71)$$

The quadratic term of the effective action reads

$$S_{\text{eff}}^{(2)}[\sigma, \pi] = \int_0^\beta d\tau \int d^3\mathbf{x} \frac{\sigma^2 + \pi^2}{4G_s} + \frac{1}{2} \text{Tr} \{ \mathcal{S} \Sigma[\sigma, \pi] \mathcal{S} \Sigma[\sigma, \pi] \}, \quad (72)$$

where Σ is defined as $\Sigma[\sigma, \pi] = \sigma + i\gamma_5 \tau \cdot \pi$. Going to the momentum space, the effective action can be evaluated as

$$\begin{aligned} S_{\text{eff}}^{(2)}[\sigma, \pi] &= \frac{1}{2} \sum_k \left[\left[\frac{1}{2G_s} - \Pi_\sigma(k) \right] \sigma(-k) \sigma(k) \right. \\ &\quad + \left[\frac{1}{2G_s} - \Pi_{\pi_0}(k) \right] \pi_0(-k) \pi_0(k) \\ &\quad + \left[\frac{1}{2G_s} - \Pi_{\pi_+}(k) \right] \pi_+(-k) \pi_-(k) \\ &\quad \left. + \left[\frac{1}{2G_s} - \Pi_{\pi_-}(k) \right] \pi_-(-k) \pi_+(k) \right], \quad (73) \end{aligned}$$

where $\pi_\pm = (\pi_1 \pm i\pi_2)/\sqrt{2}$ are the positively and negatively charged pion fields, and the polarization functions for the mesons can be evaluated as

$$\begin{aligned} \Pi_\sigma(k) &= N_c \Pi_1(k; \mu_I), & \Pi_{\pi_0}(k) &= N_c \Pi_2(k; \mu_I), \\ \Pi_{\pi_+}(k) &= N_c \Pi_3(k; \mu_I), & \Pi_{\pi_-}(k) &= N_c \Pi_4(k; \mu_I) \end{aligned} \quad (74)$$

where N_c is the color degree of freedom.

Without loss of generality, we consider the case $\mu_I > 0$ where the π_+ mesons become condensed at low temperature. The transition temperature T_c is determined by the well-known Thouless criterion

$$1 - 2G_s \Pi_{\pi_+}(k_0 = 0, \mathbf{k} = 0) \Big|_{T=T_c} = 0 \quad (75)$$

together with the gap equation for the effective quark mass m derived from the first order derivative of the thermodynamic potential with respect to m ,

$$\frac{m - m_0}{8N_c G_s m} = \int \frac{d^3\mathbf{p}}{(2\pi)^3} \frac{1 - f(E_\mathbf{p}^+) - f(E_\mathbf{p}^-)}{E_\mathbf{p}} \Big|_{T=T_c} \quad (76)$$

with $E_\mathbf{p}^\pm = E_\mathbf{p} \pm \mu_I/2$. The critical temperature as a function of isospin chemical potential is exactly the same as in Fig.1 if we replace the baryon chemical potential μ_B by the isospin chemical potential μ_I . The diquark condensed phase starts at $\mu_I = m_\pi$, and the critical temperature can be well described by[57]

$$T_c = T_0 \sqrt{1 - \left(\frac{m_\pi}{\mu_I} \right)^4}, \quad (77)$$

where T_0 is again the temperature of chiral symmetry restoration at $\mu_I = 0$.

The energy dispersions of the mesons are defined by the poles of their propagators,

$$1 - 2G_s \Pi_i(k_0 = \omega(\mathbf{k}), \mathbf{k}) = 0, \quad i = \sigma, \pi_0, \pi_+, \pi_-. \quad (78)$$

Since the sigma and neutral pion do not carry isospin charge, they do not obtain an isospin chemical potential and their masses are defined as $m_\sigma = \omega_\sigma(0)$ and $m_{\pi_0} = \omega_{\pi_0}(0)$. However, for masses of charged pions, we should subtract the corresponding isospin chemical potential from the dispersions, namely we take $m_{\pi_+} = \omega_{\pi_+}(0) + \mu_I$ and $m_{\pi_-} = \omega_{\pi_-}(0) - \mu_I$. For $\mu_I > 0$, at the transition temperature T_c , the π_+ mass is equal to the isospin chemical potential,

$$m_{\pi_+}(T_c) = \mu_I. \quad (79)$$

The numerical results for meson masses and dissociation temperatures are the same as in Figs.2 and 3 if we take the correspondence $d \leftrightarrow \pi_+$, $\bar{d} \leftrightarrow \pi_-$, $\pi \leftrightarrow \pi_0$ and $\sigma \leftrightarrow \sigma$ between the two cases.

Similarly, we can investigate the spectral function $\rho(\omega, \mathbf{k})$ for π_+ ,

$$\rho(\omega, \mathbf{k}) = -2\text{Im}D_R(\omega, \mathbf{k}), \quad (80)$$

where $D_R(\omega, \mathbf{k}) \equiv \mathcal{D}(\omega + i\eta, \mathbf{k})$ is the analytical continuation of the pion Green function $\mathcal{D}(i\omega_n, \mathbf{k})$ defined as

$$\mathcal{D}(i\omega_n, \mathbf{k}) = \frac{2G_s}{1 - 2G_s \Pi_{\pi_+}(i\omega_n, \mathbf{k})}. \quad (81)$$

The spectral function is also similar to that of diquarks in Section I. For $\mu_I < 2m$, π_+ can decay into a quark-antiquark pair only when its energy satisfies $\omega > 2m - \mu_I$, otherwise it remains a stable bound state. However, for $\mu_I > 2m$, it can decay into a quark-antiquark pair at any energy and hence becomes an unstable resonance. The numerical result for the spectral function is similar to that shown in Fig.4. In conclusion, with increasing

isospin chemical potential, the pions above the critical temperature become more and more unstable and finally disappear, which indicates a BEC-BCS crossover.

We can also define an effective non-relativistic chemical potential $\mu_N = \mu_I/2 - m$. In the deep BCS limit with $\mu_I \rightarrow \infty$, we have $m \rightarrow 0$ and $\mu_N \rightarrow \mu_I/2$. In the deep BEC limit with $\mu_I \rightarrow m_\pi$, m tends to be its vacuum value, and μ_N becomes negative and its absolute value approaches to half of the pion binding energy $2m - m_\pi$. The effective quark mass m and the chemical potential μ_N at the critical temperature are the same as in Fig.5, and the isospin chemical potential μ_I^0 for the crossover is still about 240 MeV.

B. Pion Condensation at $T < T_c$

At low enough temperature, the pions become condensed, we should introduce not only the chiral condensate $\langle \sigma \rangle$ but also the pion condensates,

$$\langle \pi_+ \rangle = \frac{\Delta_\pi}{\sqrt{2}} e^{i\theta}, \quad \langle \pi_- \rangle = \frac{\Delta_\pi}{\sqrt{2}} e^{-i\theta}. \quad (82)$$

A nonzero pion condensate $\Delta_\pi \neq 0$ means spontaneous breaking of $U_3(1)$ symmetry corresponding to the isospin charge generator I_3 . The phase factor θ indicates the direction of the $U_3(1)$ symmetry breaking. For a homogeneous superfluid, we can choose $\theta = 0$ without loss of generality. A gapless Goldstone boson will appear, which can be identified as the quantum fluctuation in the phase direction.

After a field shift $\sigma \rightarrow \langle \sigma \rangle + \sigma$ and $\pi_1 \rightarrow \Delta_\pi + \pi_1$, the effective action at zeroth order in meson fields gives the mean field thermodynamic potential,

$$\Omega = \frac{1}{\beta V} S_{\text{eff}}^{(0)} = \frac{(m - m_0)^2 + \Delta_\pi^2}{4G_s} + \frac{1}{\beta V} \ln \det \mathcal{S}_\pi^{-1}, \quad (83)$$

where \mathcal{S}_π is the quark propagator in the pion superfluid at mean field level and can be evaluated as a matrix in flavor space,

$$\mathcal{S}_\pi(p) = \begin{pmatrix} \mathcal{S}_{uu}(p) & \mathcal{S}_{ud}(p) \\ \mathcal{S}_{du}(p) & \mathcal{S}_{dd}(p) \end{pmatrix} \quad (84)$$

with the elements

$$\begin{aligned} \mathcal{S}_{uu} &= \frac{(i\nu_n + E_\mathbf{p}^-) \Lambda_+ \gamma_0}{(i\nu_n)^2 - (E_\pi^-)^2} + \frac{(i\nu_n - E_\mathbf{p}^+) \Lambda_- \gamma_0}{(i\nu_n)^2 - (E_\pi^+)^2}, \\ \mathcal{S}_{dd} &= \frac{(i\nu_n - E_\mathbf{p}^-) \Lambda_- \gamma_0}{(i\nu_n)^2 - (E_\pi^-)^2} + \frac{(i\nu_n + E_\mathbf{p}^+) \Lambda_+ \gamma_0}{(i\nu_n)^2 - (E_\pi^+)^2}, \\ \mathcal{S}_{ud} &= \frac{-i\Delta_\pi \Lambda_+ \gamma_5}{(i\nu_n)^2 - (E_\pi^-)^2} + \frac{-i\Delta_\pi \Lambda_- \gamma_5}{(i\nu_n)^2 - (E_\pi^+)^2}, \\ \mathcal{S}_{du} &= \frac{-i\Delta_\pi \Lambda_- \gamma_5}{(i\nu_n)^2 - (E_\pi^-)^2} + \frac{-i\Delta_\pi \Lambda_+ \gamma_5}{(i\nu_n)^2 - (E_\pi^+)^2}, \end{aligned} \quad (85)$$

where $E_\pi^\pm = \sqrt{(E_\mathbf{p}^\pm)^2 + \Delta_\pi^2}$ are quark energies.

The momentum distributions of quarks and anti-quarks can be calculated from the positive and negative energy components of the diagonal propagators \mathcal{S}_{uu} and \mathcal{S}_{dd} ,

$$\begin{aligned} n_u(\mathbf{p}) &= n_{\bar{d}}(\mathbf{p}) = \frac{1}{2} \left(1 - \frac{E_\mathbf{p}^-}{E_\pi^-} \right), \\ n_d(\mathbf{p}) &= n_{\bar{u}}(\mathbf{p}) = \frac{1}{2} \left(1 - \frac{E_\mathbf{p}^+}{E_\pi^+} \right). \end{aligned} \quad (86)$$

The gap equations to determine the effective quark mass m and pion condensate Δ_π can be obtained by minimizing the thermodynamic potential,

$$\frac{\partial \Omega}{\partial m} = 0, \quad \frac{\partial \Omega}{\partial \Delta_\pi} = 0. \quad (87)$$

With the explicit form of the thermodynamic potential

$$\Omega = \frac{(m - m_0)^2 + \Delta_\pi^2}{4G_s} - 4N_c \int \frac{d^3 \mathbf{p}}{(2\pi)^3} [\zeta(E_\pi^+) + \zeta(E_\pi^-)], \quad (88)$$

we obtain the explicit gap equations at zero temperature,

$$\begin{aligned} m - m_0 &= 4N_c G_s m \int \frac{d^3 \mathbf{p}}{(2\pi)^3} \frac{1}{E_\mathbf{p}} \left(\frac{E_\mathbf{p}^-}{E_\pi^-} + \frac{E_\mathbf{p}^+}{E_\pi^+} \right), \\ \Delta_\pi &= 4N_c G_s \Delta_\pi \int \frac{d^3 \mathbf{p}}{(2\pi)^3} \left(\frac{1}{E_\pi^-} + \frac{1}{E_\pi^+} \right). \end{aligned} \quad (89)$$

The numerical results for m and Δ_π are the same as in Fig.6, if we replace μ_B by μ_I . The results agree well with lattice data[10, 11, 12] at least at small isospin chemical potential. For $\mu_I < m_\pi$, the ground state is the same as the vacuum state and the isospin density keeps zero, while for $\mu_I > m_\pi$, the pion condensate and isospin density become nonzero. In the isospin chemical potential region above but close to the critical value $\mu_I = m_\pi$, the effective quark mass and pion condensate can be well described by

$$\begin{aligned} \frac{m(\mu_I)}{m(0)} &\simeq \frac{\langle \sigma \rangle(\mu_I)}{\langle \sigma \rangle(0)} = \left(\frac{m_\pi}{\mu_I} \right)^2, \\ \frac{\Delta(\mu_I)}{\langle \sigma \rangle(0)} &= \sqrt{1 - \left(\frac{m_\pi}{\mu_I} \right)^4}. \end{aligned} \quad (90)$$

The explanation of the BEC-BCS crossover at zero temperature is similar to the diquark case in Section II. For $0 < \mu_I/2 < m(\mu_I)$, the minimum of the dispersion E_π^- is at $|\mathbf{p}| = 0$ where the energy gap is $\sqrt{\mu_N^2 + \Delta_\pi^2}$. For large enough μ_I , the minimum of the dispersion is shifted to $|\mathbf{p}| \simeq \mu_I/2$ where the energy gap is Δ . The momentum distribution for u and anti- d quarks is the same as in Fig.7, which shows a BEC-BCS crossover at finite isospin chemical potential. Similar to the diquark case, the chemical potential μ_I^0 for the crossover is

$$\mu_I^0 = [2m(0)m_\pi^2]^{1/3}, \quad (91)$$

which is about $230 - 270$ MeV when the parameter values change reasonably.

The second order effective action which is quadratic in the meson fields and controls the meson behavior can be evaluated as

$$S_{\text{eff}}^{(2)}[\sigma, \pi] = \int_0^\beta d\tau \int d^3x \frac{\sigma^2 + \pi^2}{4G_s} + \frac{1}{2} \text{Tr} \{ \mathcal{S}_\pi \Sigma[\sigma, \pi] \mathcal{S}_\pi \Sigma[\sigma, \pi] \}. \quad (92)$$

In the momentum space, it is related to the meson polarizations,

$$S_{\text{eff}}^{(2)}[\sigma, \pi] = \frac{1}{2} \sum_k \left[\frac{\delta_{ij}}{2G_s} - \Pi_{ij}(k) \right] \phi_i(-k) \phi_i(k) \quad (93)$$

with $i, j = \sigma, \pi_+, \pi_-, \pi_0$, where the polarization functions Π_{ij} are defined as

$$\Pi_{ij}(k) = iN_c \int \frac{d^4p}{(2\pi)^4} \text{Tr} [\Gamma_a \mathcal{S}_\pi(p+k) \Gamma_b \mathcal{S}_\pi(p)]. \quad (94)$$

The masses of those new eigen modes in the superfluid phase are determined by the pole equation

$$\det \left[\frac{\delta_{ij}}{2G_s} - \Pi_{ij}(k_0 = M, \mathbf{k} = 0) \right] = 0. \quad (95)$$

It can be shown that the neutral pion does not mix with the other mesons and is still an eigen mode of the system, but sigma and charged pions are strongly mixed, and it is the mixing that results in a gapless Goldstone boson. From the proportional relations $\Pi_{\sigma\pi_+}, \Pi_{\sigma\pi_-} \sim m\Delta_\pi$ and $\Pi_{\pi_+\pi_-} \sim \Delta_\pi^2$ [30], the mixing between sigma and charged pions is very strong in the BEC region where m and Δ_π are both large and coexist, but can be neglected at large isospin chemical potential.

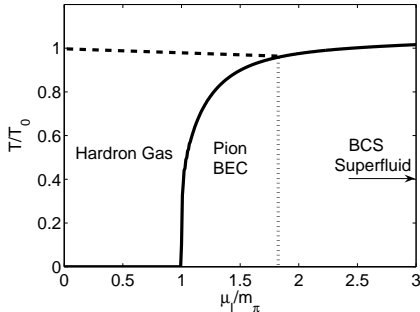


FIG. 15: The proposed phase diagram of pion condensation in the $T - \mu_I$ plane.

In summary, the phase diagram of QCD at finite isospin density is shown in Fig.15. At low temperature and low isospin chemical potential, the matter is in normal hadron gas with chiral symmetry breaking. With

increasing temperature, there should be a phase transition from hadron gas to quark gas, indicated by the thick dashed line. When the isospin chemical potential becomes larger than the pion mass in the vacuum, the pion BEC appears and keeps until another critical isospin chemical potential μ_I^0 , which is indicated by the vertical dashed line. At high enough isospin chemical potential, the matter will enter the BCS superfluid where the quark-antiquark Cooper pairs are condensed. Between the BEC and BCS, there should exist a large crossover region. Since QCD at finite isospin chemical potential can be successfully simulated on lattice, such a BEC-BCS crossover can be confirmed by measuring the quark energy gap and comparing it with the pion condensate, and the pseudogap phase can be confirmed by investigating the quark spectral function.

V. CONCLUSIONS

We have studied the BEC-BCS crossover in QCD at finite baryon or isospin density in the NJL model at quark level. We investigated the BEC-BCS crossover in two aspects: (1) Above the critical temperature of the superfluid, diquarks or mesons are stable bound states at low chemical potential but become unstable resonances at high chemical potential; (2) At zero temperature, the effective non-relativistic chemical potential, dispersions of fermion excitations and the fermion momentum distribution behavior significantly differently in the low and high chemical potential regions. The diquark BEC-BCS crossover in two color QCD at finite baryon density and the pion BEC-BCS crossover in real QCD at finite isospin density can be identified, since the quark confinement is not important in two color case. We expect that such a crossover can be confirmed in the lattice simulations, since the results from the NJL model agree quite well with the lattice data obtained so far. However, for real QCD at finite baryon density, whether there exists a diquark BEC-BCS crossover is still an open question, since the confinement in this case is quite important.

An interesting and important phenomenon we found in this paper is that the BEC-BCS crossover we discussed is not induced by simply increasing the coupling constant of the attractive interaction but by changing the corresponding charge number. During the change of the number density, the chiral symmetry restoration plays an important role in the study of BEC-BCS crossover.

When an chemical potential or fermion density mismatch between the two pairing species is turned on, the BEC-BCS crossover will be dramatically changed. The system may go from some non-uniform phases such as LOFF in the BCS region to some uniform gapless phase in the BEC region[72, 75, 76, 77, 78, 79].

Acknowledgement: We thank Dr. Meng Jin for helpful discussions. The work was supported by the grants NSFC10425810, 10435080, 10575058 and SRFDP20040003103.

APPENDIX A: POLARIZATION FUNCTIONS $\Pi_1, \Pi_2, \Pi_3, \Pi_4$

The meson and diquark polarization functions Π_1, Π_2, Π_3 and Π_4 above the critical temperature for diquark or pion condensation can be evaluated as explicit functions of temperature T and corresponding chemical potential μ ,

$$\begin{aligned}
\Pi_1(k; \mu) &= - \int \frac{d^3 \mathbf{p}}{(2\pi)^3} \left[\left(\frac{f_{\mathbf{p}}^- + f_{\mathbf{p}}^+ - f_{\mathbf{q}}^- - f_{\mathbf{q}}^+}{k_0 - E_{\mathbf{q}} + E_{\mathbf{p}}} - \frac{f_{\mathbf{p}}^- + f_{\mathbf{p}}^+ - f_{\mathbf{q}}^- - f_{\mathbf{q}}^+}{k_0 + E_{\mathbf{q}} - E_{\mathbf{p}}} \right) \mathcal{T}_-^- \right. \\
&\quad \left. + \left(\frac{2 - f_{\mathbf{p}}^- - f_{\mathbf{p}}^+ - f_{\mathbf{q}}^- - f_{\mathbf{q}}^+}{k_0 - E_{\mathbf{q}} - E_{\mathbf{p}}} - \frac{2 - f_{\mathbf{p}}^- - f_{\mathbf{p}}^+ - f_{\mathbf{q}}^- - f_{\mathbf{q}}^+}{k_0 + E_{\mathbf{q}} + E_{\mathbf{p}}} \right) \mathcal{T}_+^- \right] \\
\Pi_2(k; \mu) &= - \int \frac{d^3 \mathbf{p}}{(2\pi)^3} \left[\left(\frac{f_{\mathbf{p}}^- + f_{\mathbf{p}}^+ - f_{\mathbf{q}}^- - f_{\mathbf{q}}^+}{k_0 - E_{\mathbf{q}} + E_{\mathbf{p}}} - \frac{f_{\mathbf{p}}^- + f_{\mathbf{p}}^+ - f_{\mathbf{q}}^- - f_{\mathbf{q}}^+}{k_0 + E_{\mathbf{q}} - E_{\mathbf{p}}} \right) \mathcal{T}_+^+ \right. \\
&\quad \left. + \left(\frac{2 - f_{\mathbf{p}}^- - f_{\mathbf{p}}^+ - f_{\mathbf{q}}^- - f_{\mathbf{q}}^+}{k_0 - E_{\mathbf{q}} - E_{\mathbf{p}}} - \frac{2 - f_{\mathbf{p}}^- - f_{\mathbf{p}}^+ - f_{\mathbf{q}}^- - f_{\mathbf{q}}^+}{k_0 + E_{\mathbf{q}} + E_{\mathbf{p}}} \right) \mathcal{T}_+^+ \right] \\
\Pi_3(k; \mu) &= -2 \int \frac{d^3 \mathbf{p}}{(2\pi)^3} \left[\left(\frac{f_{\mathbf{p}}^+ - f_{\mathbf{q}}^-}{k_0 + \mu - E_{\mathbf{q}} + E_{\mathbf{p}}} - \frac{f_{\mathbf{p}}^- - f_{\mathbf{q}}^+}{k_0 + \mu + E_{\mathbf{q}} - E_{\mathbf{p}}} \right) \mathcal{T}_-^+ \right. \\
&\quad \left. + \left(\frac{1 - f_{\mathbf{p}}^- - f_{\mathbf{q}}^-}{k_0 + \mu - E_{\mathbf{q}} - E_{\mathbf{p}}} - \frac{1 - f_{\mathbf{p}}^+ - f_{\mathbf{q}}^+}{k_0 + \mu + E_{\mathbf{q}} + E_{\mathbf{p}}} \right) \mathcal{T}_+^+ \right], \\
\Pi_4(k; \mu) &= -2 \int \frac{d^3 \mathbf{p}}{(2\pi)^3} \left[\left(\frac{f_{\mathbf{p}}^- - f_{\mathbf{q}}^+}{k_0 - \mu - E_{\mathbf{q}} + E_{\mathbf{p}}} - \frac{f_{\mathbf{p}}^+ - f_{\mathbf{q}}^-}{k_0 - \mu + E_{\mathbf{q}} - E_{\mathbf{p}}} \right) \mathcal{T}_-^+ \right. \\
&\quad \left. + \left(\frac{1 - f_{\mathbf{p}}^+ - f_{\mathbf{q}}^+}{k_0 - \mu - E_{\mathbf{q}} - E_{\mathbf{p}}} - \frac{1 - f_{\mathbf{p}}^- - f_{\mathbf{q}}^-}{k_0 - \mu + E_{\mathbf{q}} + E_{\mathbf{p}}} \right) \mathcal{T}_+^+ \right], \tag{A1}
\end{aligned}$$

where we have defined $\mathbf{q} = \mathbf{p} + \mathbf{k}$, $E_{\mathbf{p}} = \sqrt{\mathbf{p}^2 + m^2}$, $f_{\mathbf{p}}^{\pm} = f(E_{\mathbf{p}} \pm \mu/2)$ with $f(x) = (1 + e^{x/T})^{-1}$ being the Fermi-Dirac distribution function and $\mathcal{T}_{\pm}^{\mp} = 1 \pm (\mathbf{p} \cdot \mathbf{q} \mp m^2) / (E_{\mathbf{p}} E_{\mathbf{q}})$.

APPENDIX B: MEISSNER MASSES SQUARED OF GLUONS

In this Appendix we list the explicit form of the Meissner masses squared m_4^2 for the 4-7th gluons and m_8^2 for the 8th gluon in two-flavor color superconductivity phase which are quoted from [80, 81],

$$m_8^2 = \frac{2g^2}{9} \int \frac{d^3 \mathbf{p}}{(2\pi)^3} [4A(\mathbf{p}) + B(\mathbf{p})], \tag{B1}$$

$$m_4^2 = \frac{2g^2}{3} \int \frac{d^3 \mathbf{p}}{(2\pi)^3} [2C(\mathbf{p}) + D(\mathbf{p})] \tag{B2}$$

with the QCD gauge coupling constant g and the functions

$$\begin{aligned}
A(\mathbf{p}) &= \frac{(E_{\Delta}^-)^2 - E_{\mathbf{p}}^- E_{\mathbf{p}}^+ + \Delta^2}{(E_{\Delta}^-)^2 - (E_{\Delta}^+)^2} \frac{f(E_1) + f(E_2) - 1}{E_{\Delta}^-} - \frac{(E_{\Delta}^+)^2 - E_{\mathbf{p}}^- E_{\mathbf{p}}^+ + \Delta^2}{(E_{\Delta}^-)^2 - (E_{\Delta}^+)^2} \frac{f(E_3) + f(E_4) - 1}{E_{\Delta}^+} + \frac{1}{E_{\mathbf{p}}}, \\
B(\mathbf{p}) &= f'(E_1) + f'(E_2) + f'(E_3) + f'(E_4), \\
C(\mathbf{p}) &= u_-^2 \left(\frac{f(E_5) - f(-E_2)}{E_5 + E_2} + \frac{f(E_7) - f(-E_1)}{E_7 + E_1} \right) + v_-^2 \left(\frac{f(E_5) - f(E_1)}{E_5 - E_1} + \frac{f(E_7) - f(E_2)}{E_7 - E_2} \right) \\
&\quad + u_+^2 \left(\frac{f(E_6) - f(-E_3)}{E_6 + E_3} + \frac{f(E_8) - f(-E_4)}{E_8 + E_4} \right) + v_+^2 \left(\frac{f(E_6) - f(E_4)}{E_6 - E_4} + \frac{f(E_8) - f(E_3)}{E_8 - E_3} \right) + \frac{2}{E_{\mathbf{p}}}, \\
D(\mathbf{p}) &= u_-^2 \left(\frac{f(E_6) - f(E_2)}{E_6 - E_2} + \frac{f(E_8) - f(E_1)}{E_8 - E_1} \right) + v_-^2 \left(\frac{f(E_6) - f(-E_1)}{E_6 + E_1} + \frac{f(E_8) - f(-E_2)}{E_8 + E_2} \right) \\
&\quad + u_+^2 \left(\frac{f(E_5) - f(E_3)}{E_5 - E_3} + \frac{f(E_7) - f(E_4)}{E_7 - E_4} u_+^2 \right) + v_+^2 \left(\frac{f(E_5) - f(-E_4)}{E_5 + E_4} + \frac{f(E_7) - f(-E_3)}{E_7 + E_3} \right), \tag{B3}
\end{aligned}$$

where the quark energies are defined as

$$\begin{aligned} E_1 &= E_{\Delta}^- - \delta\mu, & E_2 &= E_{\Delta}^- + \delta\mu, & E_3 &= E_{\Delta}^+ - \delta\mu, & E_4 &= E_{\Delta}^+ + \delta\mu, \\ E_5 &= E_b^+ - \delta\mu, & E_6 &= E_b^- + \delta\mu, & E_7 &= E_b^+ + \delta\mu, & E_8 &= E_b^- - \delta\mu \end{aligned} \quad (B4)$$

with the chemical potential difference $\delta\mu$ between u and d quarks and E_{Δ}^{\pm} and E_b^{\pm} being listed in Section III, the coherent coefficients u_{\pm}^2 and v_{\pm}^2 are defined as $u_{\pm}^2 = (1 + E_{\mathbf{p}}^{\pm}/E_{\Delta}^{\pm})/2$ and $v_{\pm}^2 = (1 - E_{\mathbf{p}}^{\pm}/E_{\Delta}^{\pm})/2$, and $f'(x)$ is the first order derivative of the Fermi-Dirac distribution function. Note that we have added the terms $1/E_{\mathbf{p}}$ to A and $2/E_{\mathbf{p}}$ to C to cancel the vacuum contribution. In this way the Meissner masses squared are guaranteed to be zero in the normal phase with $\Delta = 0$.

[1] For instance, see *Quark-Gluon Plasma*, ed. R.C.Hwa (world Scientific, Singapore, 1990)

[2] M.Alford, K.Rajagopal, and F.Wilczek, Phys. Lett. **B422**, 247(1998)

[3] R.Rapp, T.Schäfer, E.V. Shuryak and M. Velkovsky, Phys.Rev.Lett.**81**, 53(1998)

[4] D.T.Son and M.A.Stephanov, Phys.Rev.Lett.**86**, 592(2001)

[5] F.Karsch, Lect. Notes Phys. **583**, 209(2002)

[6] S.Hands, I.Montvay, S.Morrison, M.Oevers, L.Scorzato and J.Skullerud, Eur.Phys.J.**C17**, 285(2000)

[7] S.Hands, I.Montvay, L.Scorzato and J.Skullerud, Eur.Phys.J.**C22**, 451(2001)

[8] J.B.Kogut, D.Toublan and D.K.Sinclair, Phys.Lett.**B514**, 77(2001)

[9] S.Hands, S.Kim and J.Skullerud, PoS LAT2005, 149(2005); hep-lat/0508027

[10] J.B.Kogut, D.K.Sinclair, Phys.Rev.**D66**, 034505(2002)

[11] J.B.Kogut, D.K.Sinclair, Phys.Rev.**D66**, 014508(2002)

[12] J.B.Kogut, D.K.Sinclair, Phys.Rev.**D70**, 094501(2004)

[13] J.B.Kogut, M.A.Stephanov and D.Toublan, Phys.Lett.**B464**, 183(1999)

[14] J.B.Kogut, M.A.Stephanov, D.Toublan, J.J.M.Verbaarschot and A. Zhitnitsky, Nucl.Phys.**B582**, 477(2000)

[15] J.B.Kogut and D.Toublan, Phys.Rev.**D64**, 034007(2001)

[16] K.Splittorff, D.T.Son and M.A.Stephanov, Phys.Rev. **D64** 016003(2001)

[17] J.T.Lenaghan, F.Sannino, K.Splittorff, Phys.Rev. **D65**, 054002(2002)

[18] K.Splittorff, D.Toublan, J.J.M.Verbaarschot, Nucl.Phys.**B620**, 290(2002)

[19] Michael C. Birse, Thomas D. Cohen and Judith A. McGovern, Phys.Lett. **B516** 27(2001)

[20] M.Lowe and C.Villavicencio, Phys.Rev.**D67**, 074034(2003); Phys.Rev.**D70**, 074005(2004)

[21] B.J.Harrington and H.K.Shepard, Phys.Rev.**D16**, 3437(1977)

[22] J.O.Andersen, hep-ph/0609020

[23] H.Mao, N.Petropoulos, S.Shu, W.Zhao, J. Phys. **G32**, 2187(2006)

[24] D.Toublan and J.B.Kogut, Phys.Lett. **B564**, 212(2003)

[25] A.Barducci, R.Casalbuoni, G.Pettini, L.Ravagli, Phys.Rev. **D69**, 096004(2004)

[26] A.Barducci, R.Casalbuoni, G.Pettini, L.Ravagli, Phys.Rev. **D71**, 016011(2005)

[27] M.Frank, M.Buballa and M.Oertel, Phys.Lett. **B562**, 221(2003)

[28] C.Ratti and W.Weise, Phys.Rev.**D70**, 054013(2004)

[29] L.He and P.Zhuang, Phys.Lett.**B615**, 93(2005); L.He, M.Jin and P.Zhuang, hep-ph/0503249

[30] L.He, M.Jin and P.Zhuang, Phys.Rev.**D71**, 116001(2005)

[31] H.J.Warringa, D.Boer and J.O.Andersen, Phys.Rev.**D72**, 014015(2005)

[32] B.Klein, D.Toublan and J.J.M.Verbaarschot, Phys.Rev. **D68**, 014009(2003)

[33] B.Klein, D.Toublan and J.J.M.Verbaarschot, Phys.Rev. **D72**, 015007(2005)

[34] A.Barducci, R.Casalbuoni, G.Pettini, L.Ravagli, Phys.Lett. **B564**, 217(2003)

[35] Y.Nishida, Phys.Rev.**D69**, 094501(2004)

[36] Z.Zhang, L.Chang and Y.Liu, hep-ph/0603252

[37] D.M.Eagles, Phys.Rev.**186**, 456(1969)

[38] A.J.Leggett, in *Modern trends in the theory of condensed matter*, edited by A.Pekalski and J.Przystawa (Springer-Verlag, Berlin, 1980)

[39] P.Nozieres and S.Schmitt-Rink, J.Low.Temp.Phys **59**, 195(1985)

[40] C.A.R.Sa de Melo, M.Randeria and J.R.Engelbrecht, Phys.Rev.Lett.**71**, 3202(1993)

[41] J.R.Engelbrecht, M.Randeria and C.A.R.Sa de Melo, Phys.Rev.**B55**, 15153(1997)

[42] Q.Chen, J.Stajic, S.Tan and K.Levin, Phys.Rept.412, 1(2005)

[43] E.Babaev, Phys.Rev.**D62**, 074021(2000); Int.J.Mod.Phys.**A16**, 1175(2001)

[44] Y.Nishida and H.Abuiki, Phys.Rev. **D72**, 096004(2005)

[45] H.Abuiki, hep-ph/0605081

[46] J.Deng, A.Schmitt and Q.Wang, nucl-th/0611097

[47] M.Baldo, U.Lombardo and P.Schuck, Phys.Rev.**C52**, 975(1995)

[48] N.Andrenacci, A.Perali, P.Pieri and G.C.Strinati, Phys.Rev.**B60**, 12410(1999)

[49] Nambu and G.Jona-Lasinio, Phys.Rev.**122**, 345(1961); **124**, 246(1961)

[50] U.Vogl and Weise, Prog. Part. and Nucl. Phys. **27**, 195(1991)

[51] S.P.Klevansky, Rev.Mod.Phys.**64**, 649(1992)

[52] M.K.Volkov, Phys.Part.Nucl.**24**, 35(1993)

[53] T.Hatsuda and T.Kunihiro, Phys.Rep.**247**, 221(1994)

[54] M.Buballa, Phys.Rept.407, 205(2005)

[55] J.Hufner, S.P.Klevansky, P.Zhuang and H.Voss,

Ann.Phys(N.Y)**234**, 225(1994)

[56] P.Zhuang, J.Hufner, S.P.Klevansky, Nucl.Phys.**A576**,525(1994)

[57] K.Splittorff, hep-lat/0505001

[58] L.He, M.Jin and P.Zhuang, hep-ph/0511300

[59] D.Ebert, K.G.Klimenko and V.L.Yudichev, Phys.Rev.**C72**, 015201(2005); Phys.Rev.**D72**, 056007(2005)

[60] P.Zhuang, hep-ph/0503250

[61] M.Huang, P.Zhuang and W.Chao, Phys.Rev.**D65**, 076012(2002)

[62] M.Kitazawa, T.Koide, T.Kunihiro and Y.Nemoto, Prog.Theor.Phys.108, 929(2002)

[63] T.Hatsuda, M.Tachibana, N.Yamamoto and G.Baym, Phys.Rev.Lett.97, 122001(2006)

[64] M.Huang,P.Zhuang and W.Chao, Phys.Rev.**D67**, 065015(2003)

[65] I.Shovkovy and M.Huang, Phys.Lett.**B564**, 205(2003)

[66] M.Huang and I.Shovkovy, Phys.Rev. **D70**, 051501(R)(2004)

[67] I.Giannakis and H.Ren, Phys.Lett.**B611**, 137(2005); Nucl.Phys.**B723**, 255(2005)

[68] I.Giannakis, D.Hou and H.Ren, Phys.Lett.**B631**, 16(2005)

[69] L.He, M.Jin and P.Zhuang, Phys.Rev.**B73**, 214527(2006)

[70] M.Kitazawa, D.Rischke and A.Shovkovy, Phys.Lett.**B637**, 367(2006)

[71] L.He, M.Jin and P.Zhuang, Phys.Rev.**D74**, 056007(2006)

[72] C.H.Pao, S.Wu and S.K.Yip, Phys.Rev.**B73**, 132506(2006)

[73] D.T.Son and M.A.Stephanov, Phys.Rev. **A74**, 013614(2006)

[74] E.Gubankova, A.Schmitt and F.Wilczek, Phys.Rev.**B74**, 064505(2006)

[75] D.E.Sheehey and L.Radzihovsky, Phys.Rev.Lett.**96**,060401(2006); cond-mat/0607803

[76] H.Hu and X.-J. Liu, Phys.Rev.**A73**, 051603(R)(2006)

[77] L.He, M.Jin and P.Zhuang, Phys.Rev.**D74**, 036005(2006)

[78] M.Jin, L.He and P.Zhuang, nul-th/0609065

[79] P.Pieri, D.Neilson, G.C.Strinati, cond-mat/0610311

[80] M.Huang and I.Shovkovy, Phys.Rev. **D70**, 094030(2004)

[81] L.He, M.Jin and P.Zhuang, Phys. Rev. **D75**, 036003(2007)